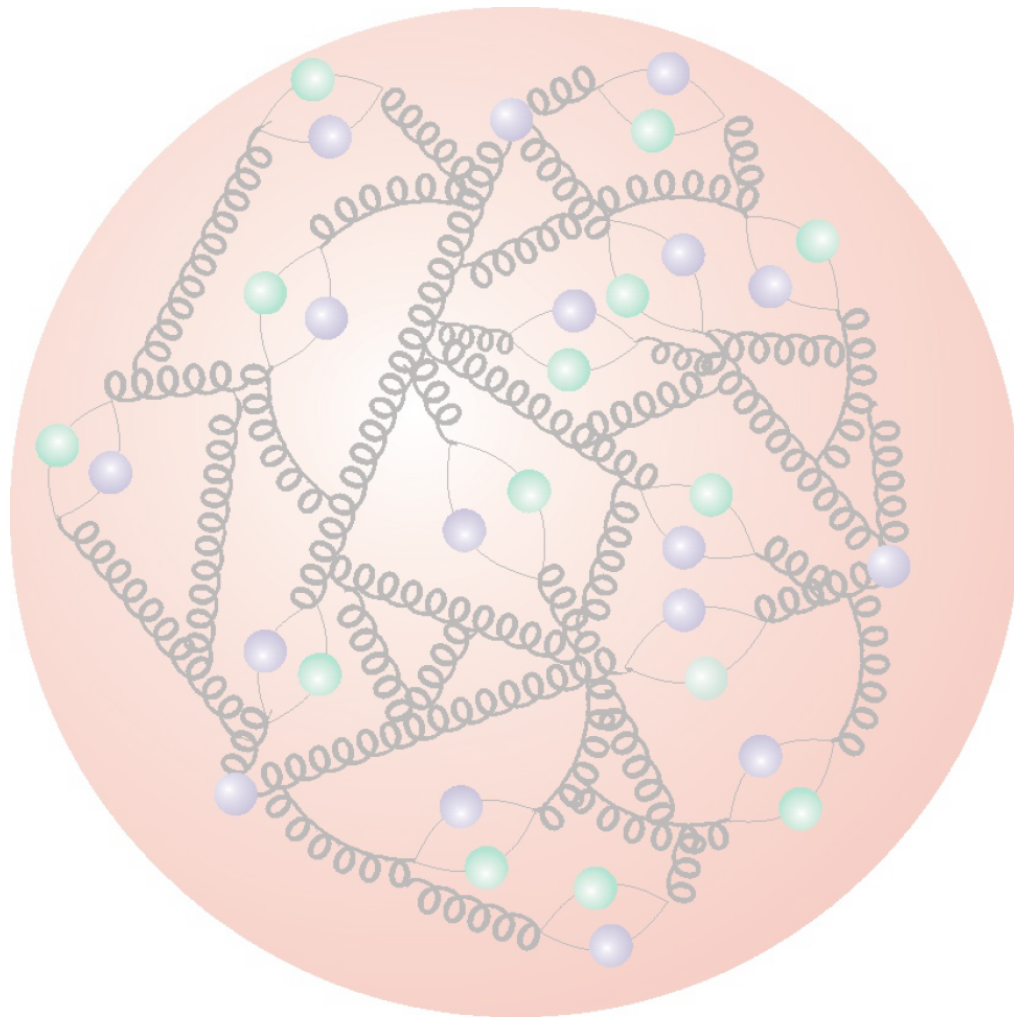


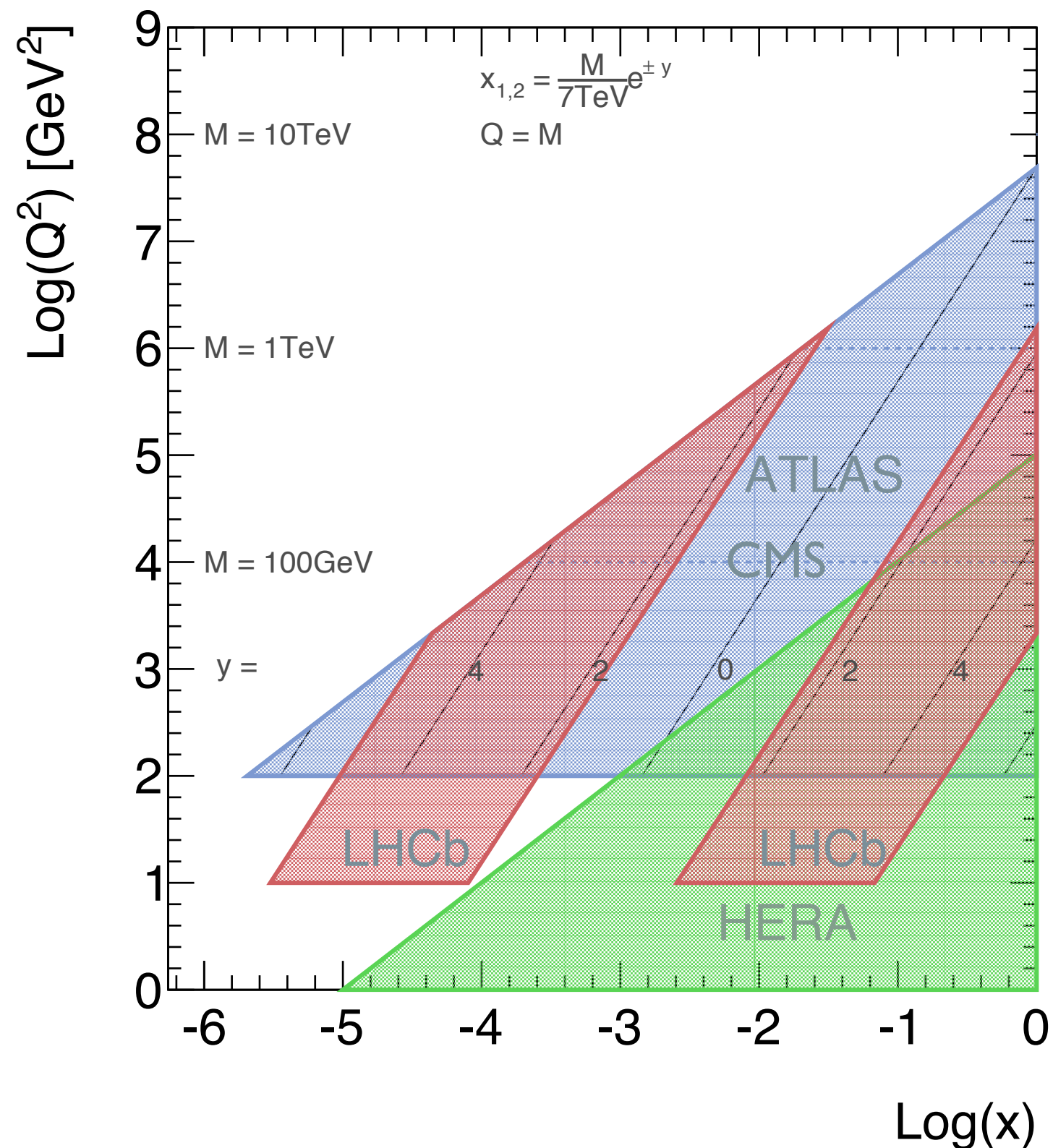
New DIS & Collider Results



- Introduction
- HERA-II Updates
- H1 NC/CC $e^\pm p$
- ZEUS NC $e^+ p$
- HERAPDF Plans
- LHC Constraints

Eram Rizvi

International Workshop on Neutrino-Nucleus Interactions
Rio de Janeiro – 23rd Oct. 2012



Final H1 & ZEUS structure function data published

New LHC data being rapidly published

Searches for high mass states require precision knowledge at high x

For central production $x=x_1=x_2$

$$M = x^2 \sqrt{s}$$

→ $M > 1 \text{ TeV}$ probes $x > 0.1$

DGLAP evolution allows predictions to be made

High x predictions rely on

- data (DIS / fixed target)
- sum rules
- behaviour of PDFs as $x \rightarrow 1$

Low x region important for high energy cosmic rays

$$\frac{d\sigma_{NC}^{\pm}}{dx dQ^2} = \frac{2\pi\alpha^2}{x} \left[\frac{1}{Q^2} \right]^2 \left[Y_+ \tilde{F}_2 \mp Y_- x \tilde{F}_3 - y^2 \tilde{F}_L \right]$$

$$\frac{d\sigma_{CC}^{\pm}}{dx dQ^2} = \frac{G_F^2}{4\pi x} \left[\frac{M_W^2}{M_W^2 + Q^2} \right]^2 \left[Y_+ \tilde{W}_2^{\pm} \mp Y_- x \tilde{W}_3^{\pm} - y^2 \tilde{W}_L^{\pm} \right]$$

$$Y_{\pm} = 1 \pm (1 - y)^2$$

$$\tilde{F}_2 \propto \sum (xq_i + x\bar{q}_i)$$

Dominant contribution

$$x\tilde{F}_3 \propto \sum (xq_i - x\bar{q}_i)$$

Only sensitive at high $Q^2 \sim M_Z^2$

$$\tilde{F}_L \propto \alpha_s \cdot xg(x, Q^2)$$

Only sensitive at low Q^2 and high y

The NC reduced cross section defined as:

$$\tilde{\sigma}_{NC}^{\pm} = \frac{Q^2 x}{2\alpha\pi^2} \frac{1}{Y_+} \frac{d^2\sigma^{\pm}}{dx dQ^2}$$

$$\tilde{\sigma}_{NC}^{\pm} \sim \tilde{F}_2 \mp \frac{Y_-}{Y_+} x\tilde{F}_3$$

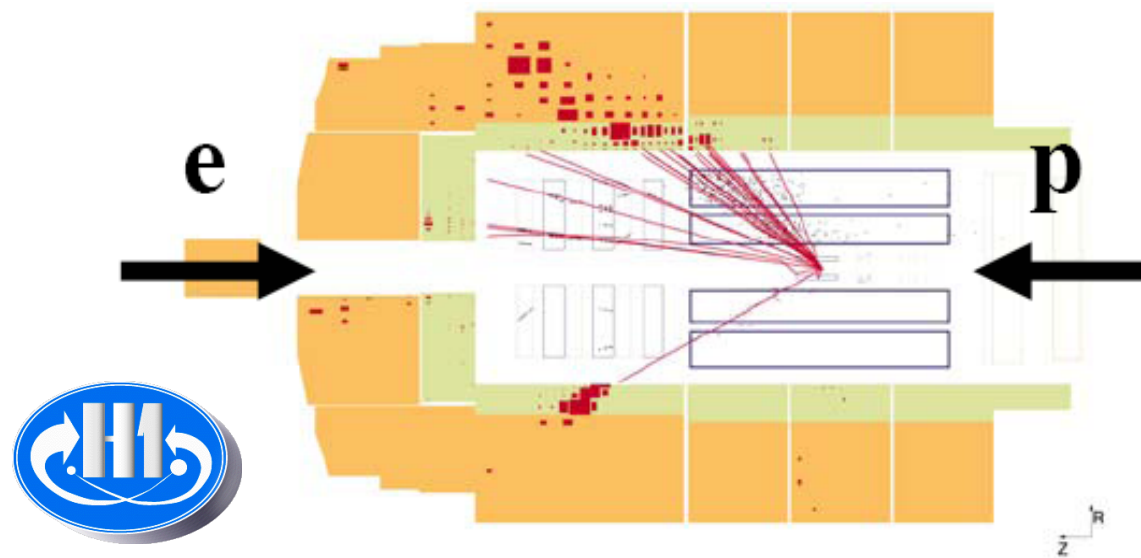
The CC reduced cross section defined as:

$$\sigma_{CC}^{\pm} = \frac{2\pi x}{G_F^2} \left[\frac{M_W^2 + Q^2}{M_W^2} \right]^2 \frac{d\sigma_{CC}^{\pm}}{dx dQ^2}$$

$$\frac{d\sigma_{CC}^{\pm}}{dx dQ^2} = \frac{1}{2} \left[Y_+ W_2^{\pm} \mp Y_- x W_3^{\pm} - y^2 W_L^{\pm} \right]$$

similarly for pure weak CC analogues:

$$W_2^{\pm}, xW_3^{\pm} \text{ and } W_L^{\pm}$$



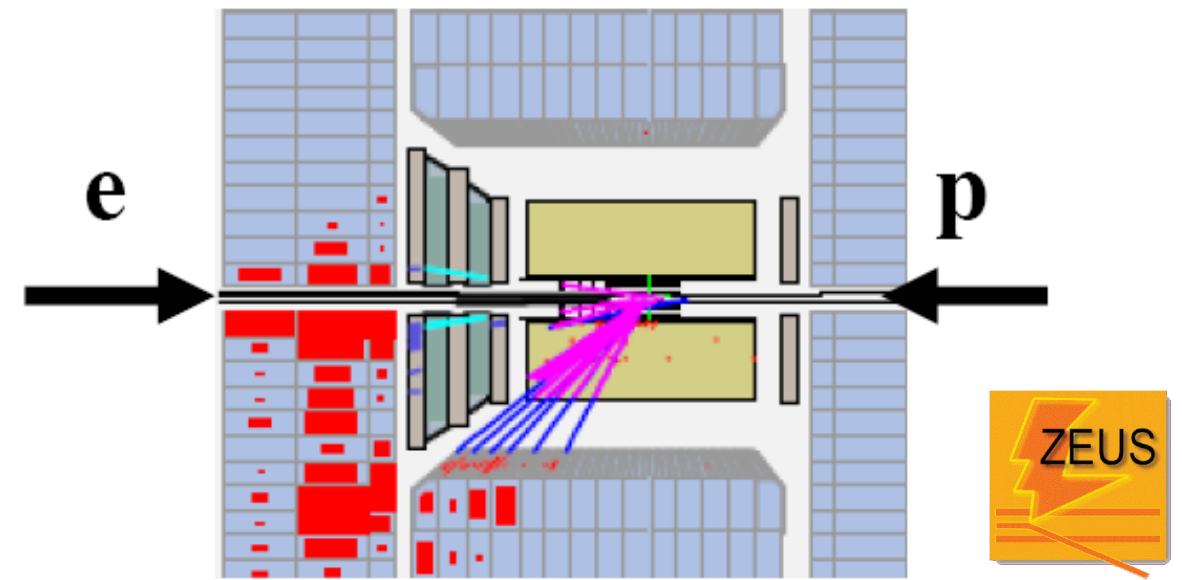
Neutral current event selection:

High P_T isolated scattered lepton
 Suppress huge photo-production background by imposing longitudinal energy-momentum conservation

Kinematics may be reconstructed in many ways:
 energy/angle of hadrons & scattered lepton
 provides excellent tools for sys cross checks

Removal of scattered lepton provides a
 high stats “pseudo-charged current sample”
 Excellent tool to cross check CC analysis

Final selection: $\sim 10^5$ events per sample at high Q^2
 $\sim 10^7$ events for $10 < Q^2 < 100 \text{ GeV}^2$



Charged current event selection:

Large missing transverse momentum (neutrino)
 Suppress huge photo-production background
 Topological finders to remove cosmic muons

Kinematics reconstructed from hadrons
 Final selection: $\sim 10^3$ events per sample

HERA-I operation 1993-2000

$E_e = 27.6 \text{ GeV}$

$E_p = 820 / 920 \text{ GeV}$

$\int \mathcal{L} \sim 110 \text{ pb}^{-1}$ per experiment

HERA-II operation 2003-2007

$E_e = 27.6 \text{ GeV}$

$E_p = 920 \text{ GeV}$

$\int \mathcal{L} \sim 330 \text{ pb}^{-1}$ per experiment

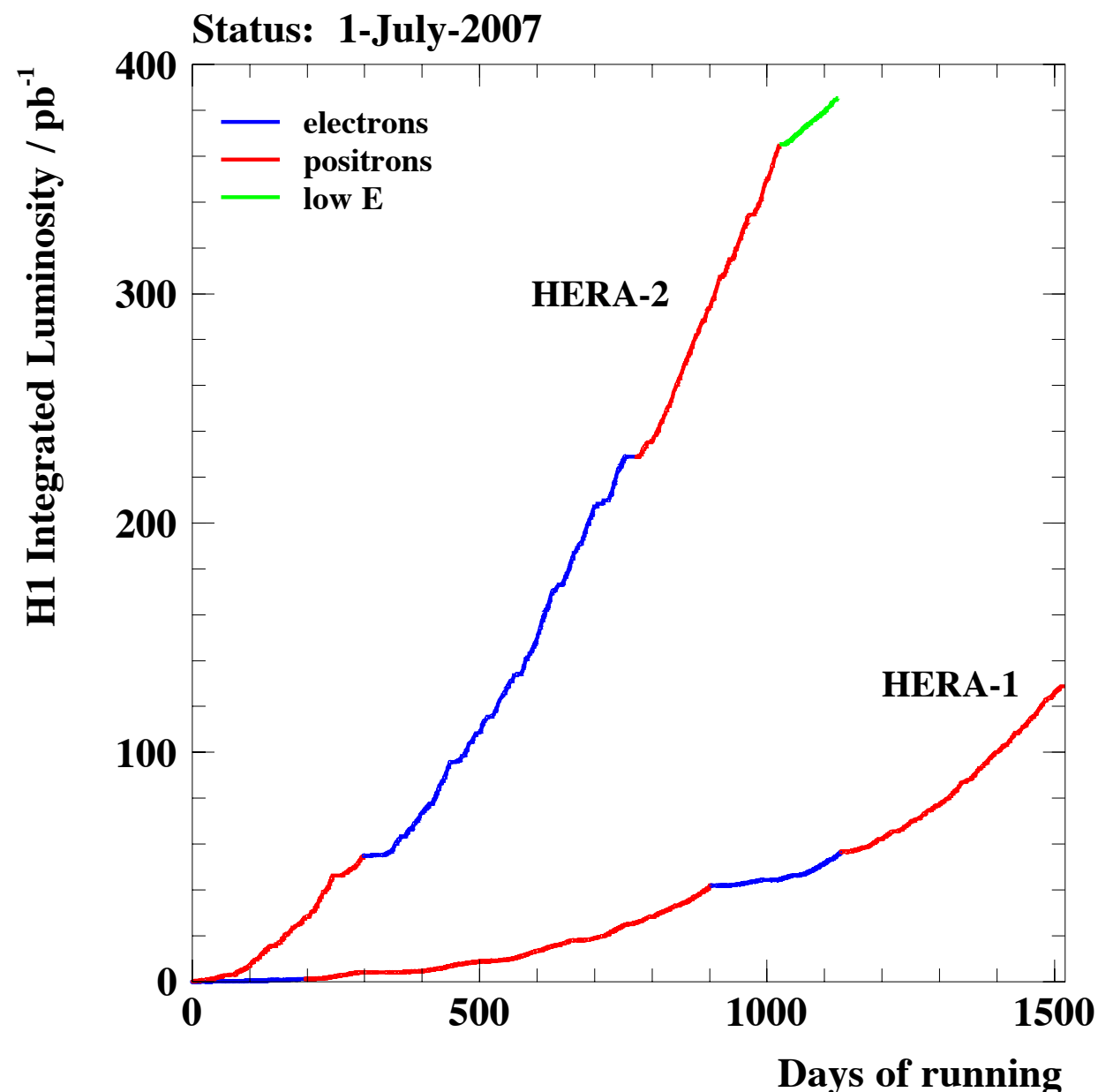
Longitudinally polarised leptons

Low Energy Run 2007

$E_e = 27.6 \text{ GeV}$

$E_p = 575 \text{ \& } 460 \text{ GeV}$

Dedicated F_L measurement



breakdown of HERA-II data samples

| | R | L |
|--------|--|--|
| e^-p | $\mathcal{L} = 47.3 \text{ pb}^{-1}$ $P_e = (+36.0 \pm 1.0)\%$ | $\mathcal{L} = 104.4 \text{ pb}^{-1}$ $P_e = (-25.8 \pm 0.7)\%$ |
| e^+p | $\mathcal{L} = 101.3 \text{ pb}^{-1}$ $P_e = (+32.5 \pm 0.7)\%$ | $\mathcal{L} = 80.7 \text{ pb}^{-1}$ $P_e = (-37.0 \pm 0.7)\%$ |

Up till now HERA-II datasets only partially published

| | | |
|----------------|----------------------|-------------------------|
| ZEUS CC e^-p | 175 pb ⁻¹ | EPJ C 61 (2009) 223-235 |
| ZEUS CC e^+p | 132 pb ⁻¹ | EPJ C 70 (2010) 945-963 |
| ZEUS NC e^-p | 170 pb ⁻¹ | EPJ C 62 (2009) 625-658 |
| ZEUS NC e^+p | 135 pb ⁻¹ | ZEUS-prel-11-003 |
| H1 CC e^-p | 149 pb ⁻¹ | H1prelim-09-043 |
| H1 CC e^+p | 180 pb ⁻¹ | H1prelim-09-043 |
| H1 NC e^-p | 149 pb ⁻¹ | H1prelim-09-042 |
| H1 NC e^+p | 180 pb ⁻¹ | H1prelim-09-042 |



HERA-II datasets
Combined in HERAPDF1.5
(except ZEUS NC e^+p)

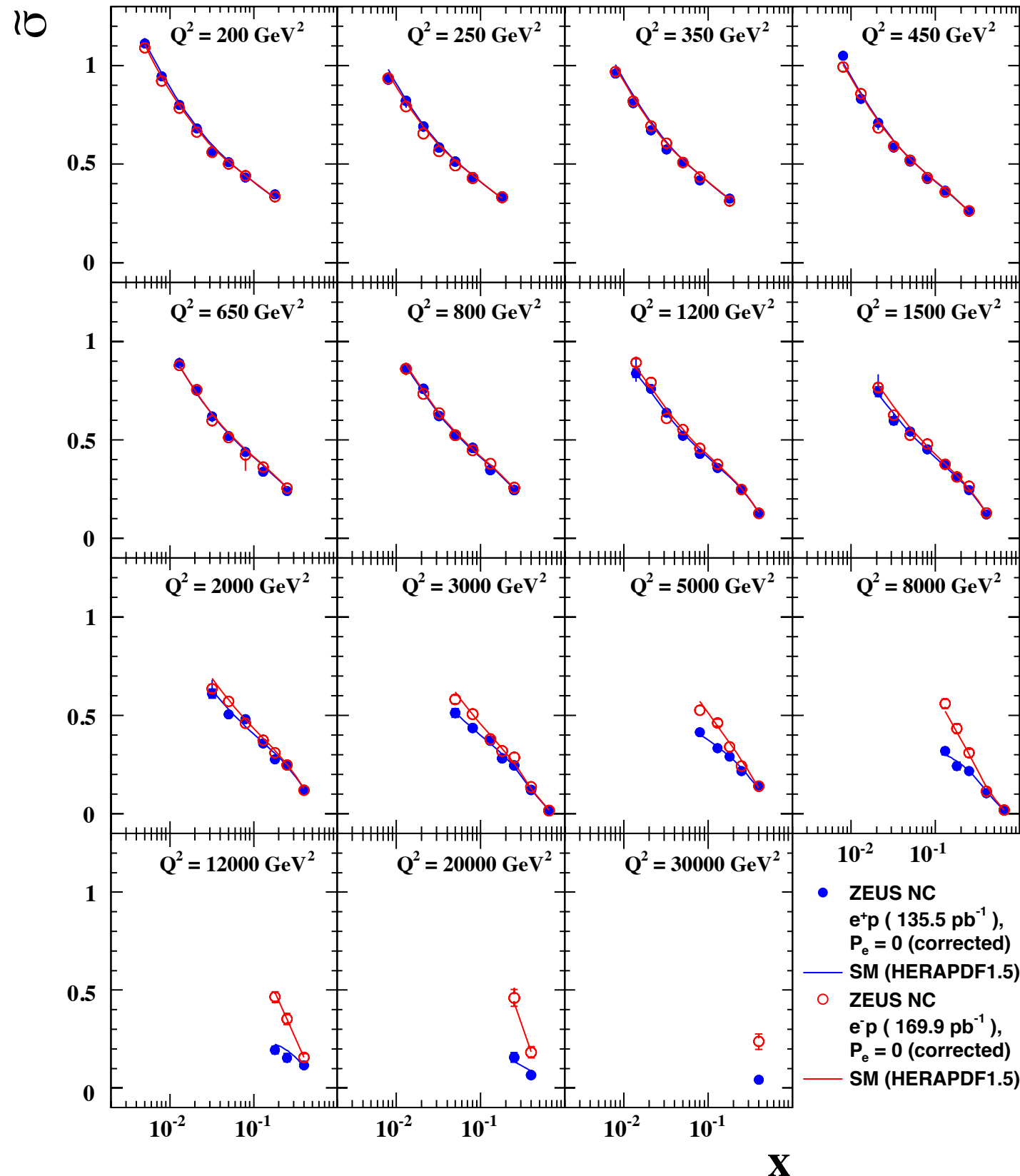


| | | |
|----------------|----------------------|-------------------------|
| ZEUS CC e^-p | 175 pb ⁻¹ | EPJ C 61 (2009) 223-235 |
| ZEUS CC e^+p | 132 pb ⁻¹ | EPJ C 70 (2010) 945-963 |
| ZEUS NC e^-p | 170 pb ⁻¹ | EPJ C 62 (2009) 625-658 |
| ZEUS NC e^+p | 135 pb ⁻¹ | arXiv:1208.6138 |
| H1 CC e^-p | 149 pb ⁻¹ | arXiv:1206.7007 |
| H1 CC e^+p | 180 pb ⁻¹ | |
| H1 NC e^-p | 149 pb ⁻¹ | |
| H1 NC e^+p | 180 pb ⁻¹ | |

Complete the analyses of HERA high Q^2 inclusive structure function data

New published data increase $\int \mathcal{L}$ by
 ~ factor 3 for e^+p
 ~ factor 10 for e^-p
 much improved systematic uncertainties

ZEUS



Z^0 contribution enhances as Q^2 increases

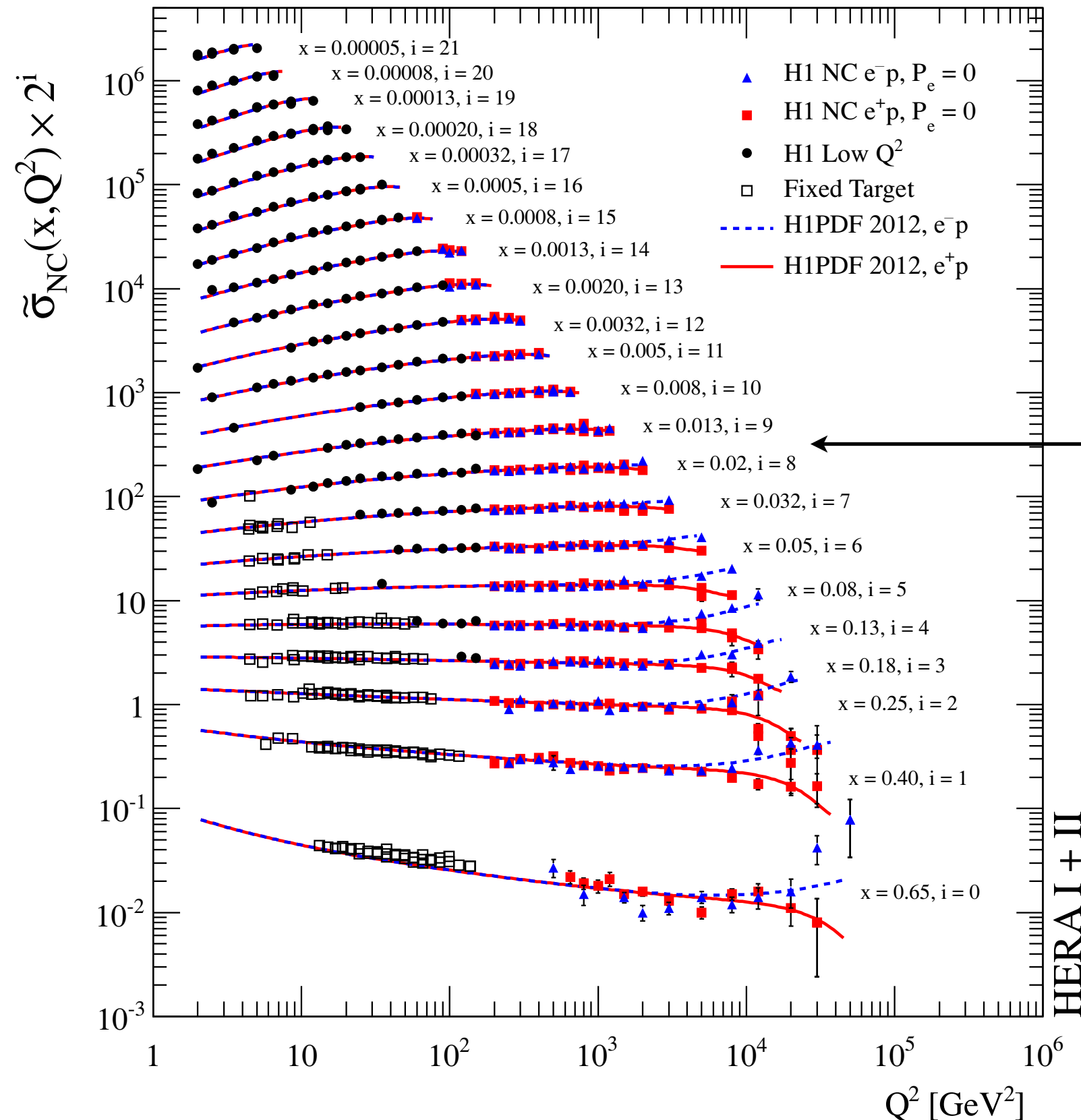
Final measurement of ZEUS NC e^+p data

Shown here for $P=0$

Polarised measurements also available

Compared to published NC e^-p data

H1 Collaboration



H1 precision 1.5% for $Q^2 < 500$ GeV²
 \Rightarrow factor 2 reduction in error wrt HERA-I

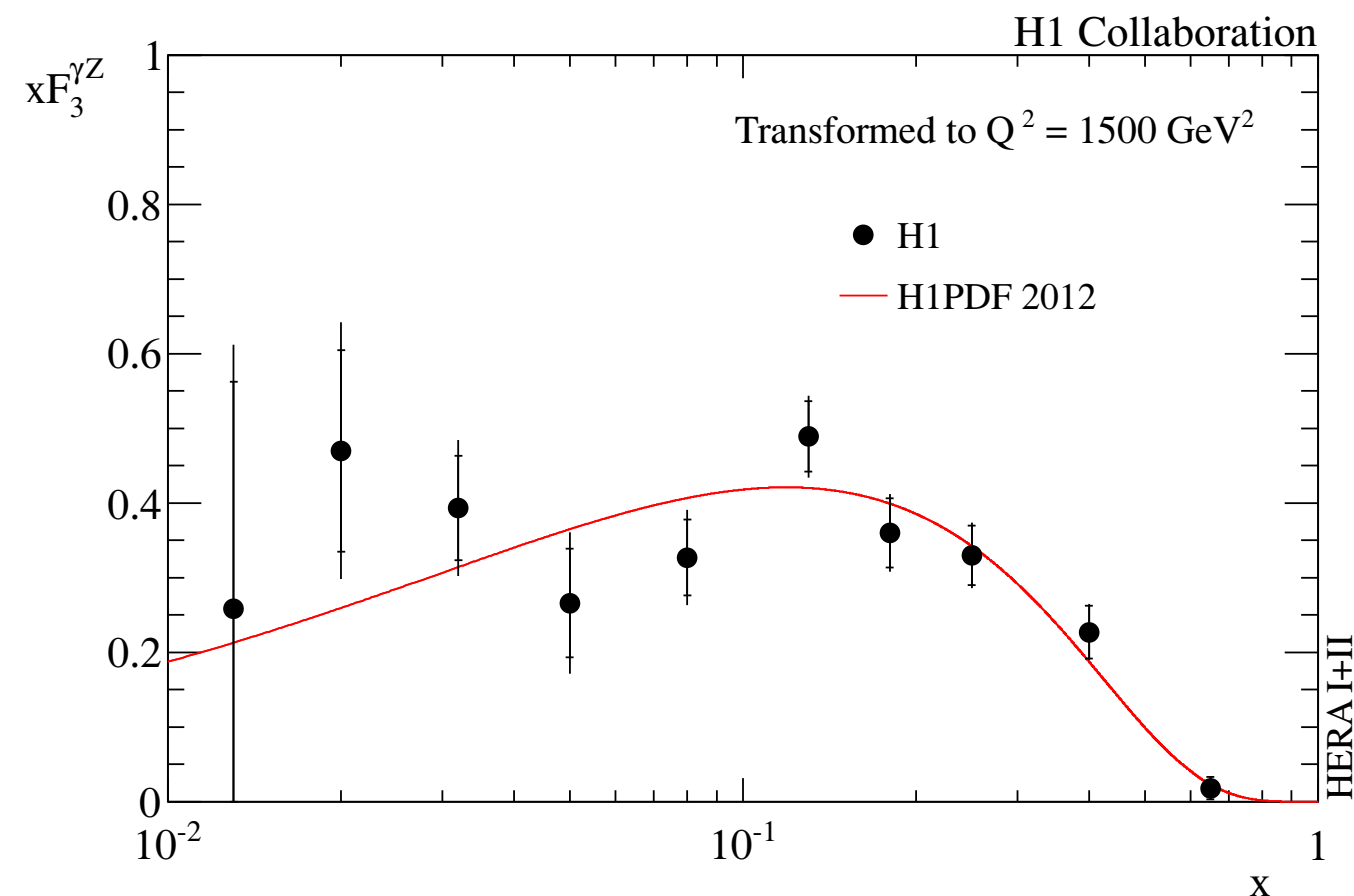
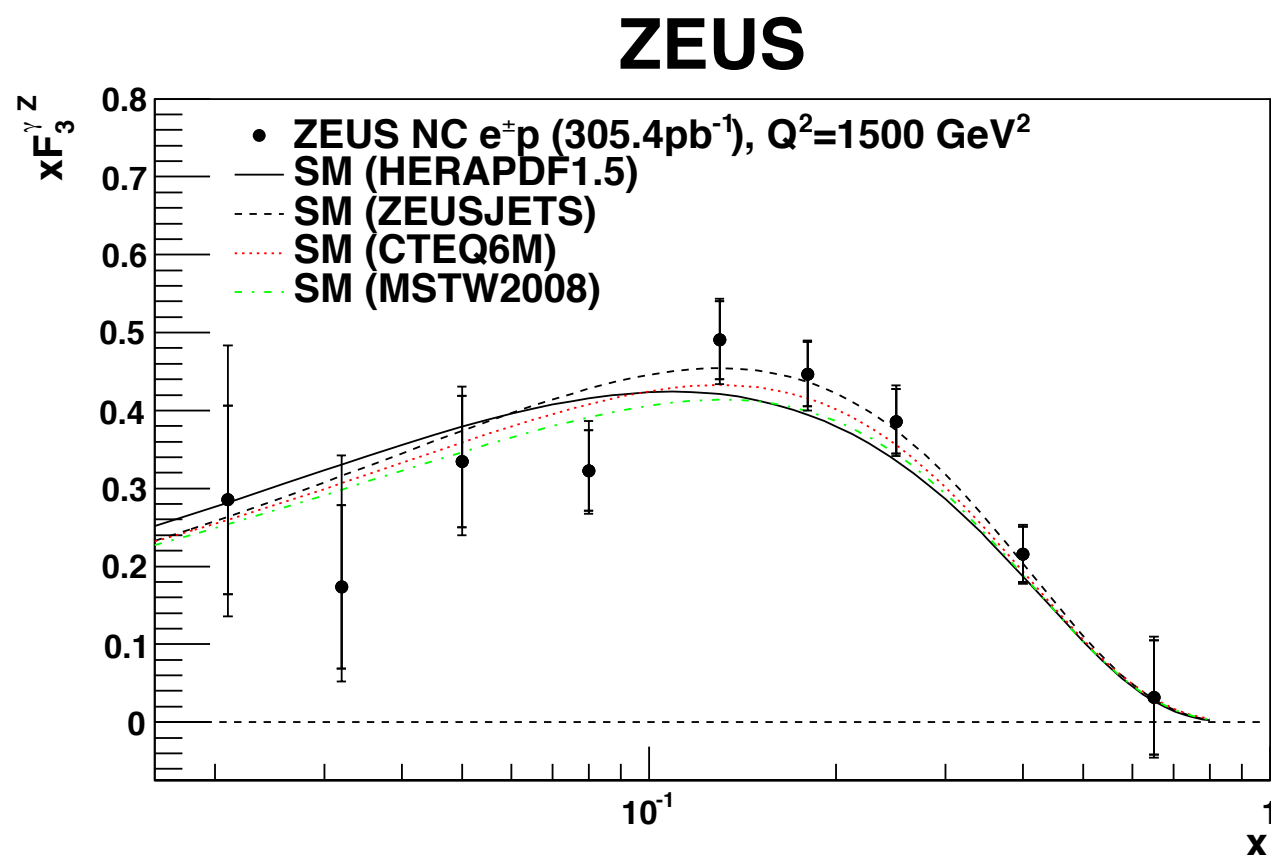
Statistics limited at higher Q^2 and high x

Extended reach at high x compared to H1 preliminary data

This x region is the 'sweet spot'
 High precision with long Q^2 lever arm
 x -range relevant for Higgs production

Combination of high Q^2 data
 HERA-I and HERA-II

Larger HERA-II luminosity
 \rightarrow improved precision at high x / Q^2



At high Q^2 $x\tilde{F}_3$ arises due to Z^0 effects
 enhanced e^- cross section wrt e^+
 Difference is $x\tilde{F}_3$
 Sensitive to valence PDFs

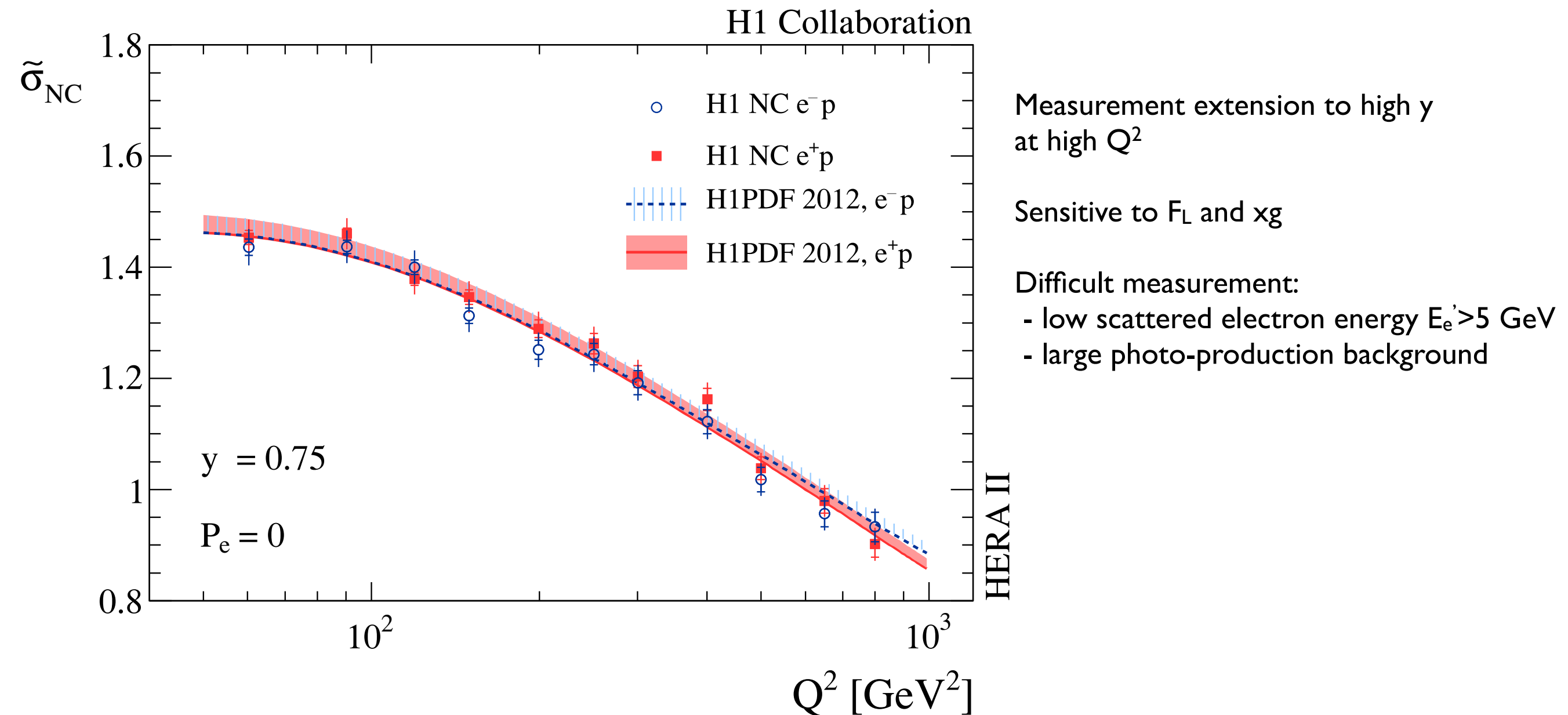
$$x\tilde{F}_3 = \frac{Y_+}{2Y_-} (\tilde{\sigma}_{NC}^- - \tilde{\sigma}_{NC}^+) \approx a_e \chi_Z xF_3^{\gamma Z}$$

$$x\tilde{F}_3 \propto \sum (xq_i - x\bar{q}_i)$$

H1 measure integral of $x\tilde{F}_3^{\gamma Z}$ - validate sumrule:

$$\int_{0.016}^{0.725} dx F_3^{\gamma Z}(x, Q^2 = 1500 \text{ GeV}^2) = 1.22 \pm 0.09(\text{stat}) \pm 0.07(\text{syst})$$

NLO integral predicted to
 be $5/3 + \mathcal{O}(\alpha_s/\pi) = 1.16$



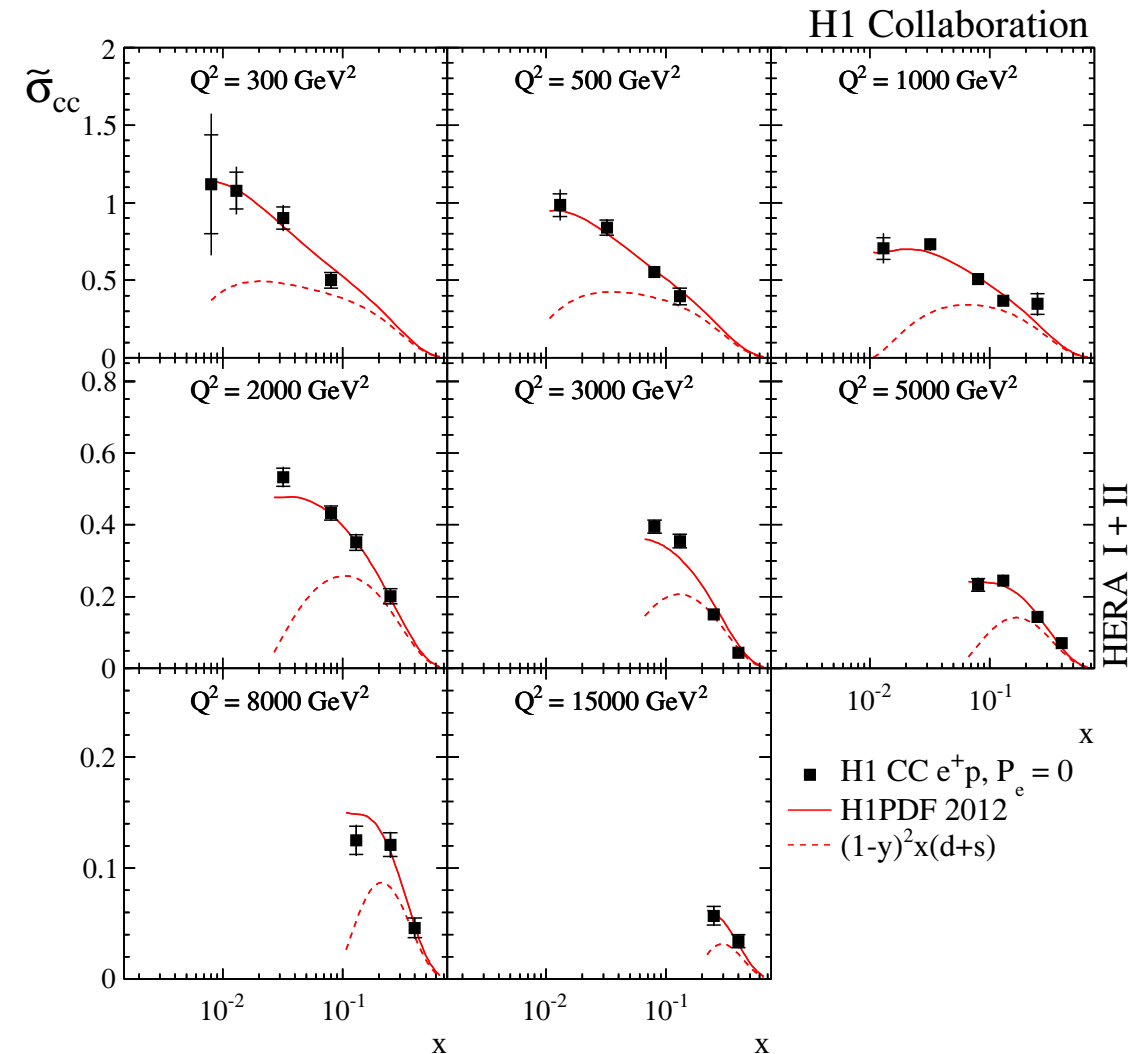
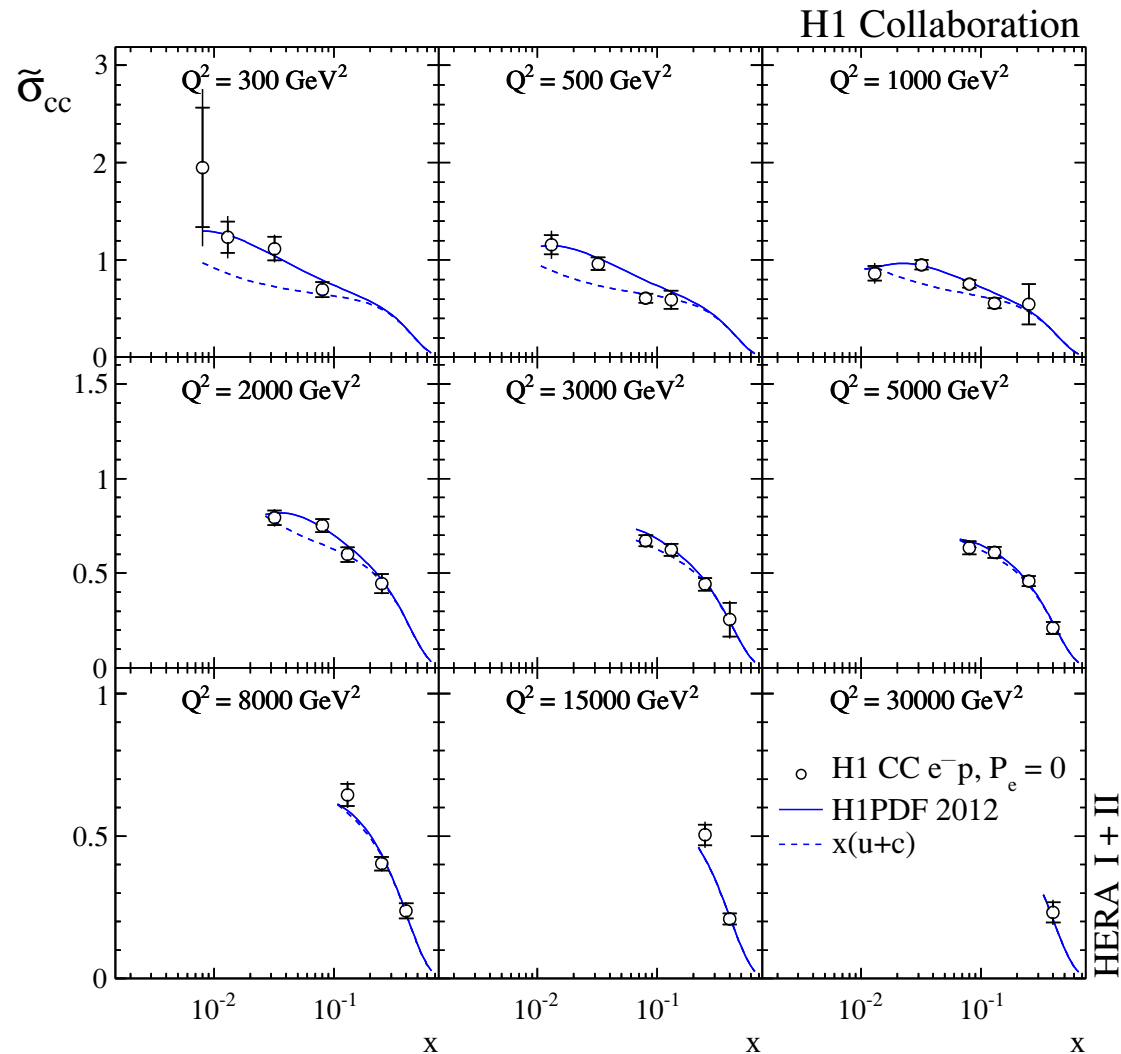
Total uncertainty reduced by factor 2:
 HERA-I ~4%
 HERA-II ~2%

Electron scattering

$$\frac{d^2\sigma_{CC}^-}{dx dQ^2} = \frac{G_F^2}{2\pi} \left(\frac{M_W^2}{M_W^2 + Q^2} \right)^2 \left[(u + c) + (1 - y)^2 (\bar{d} + \bar{s}) \right]$$

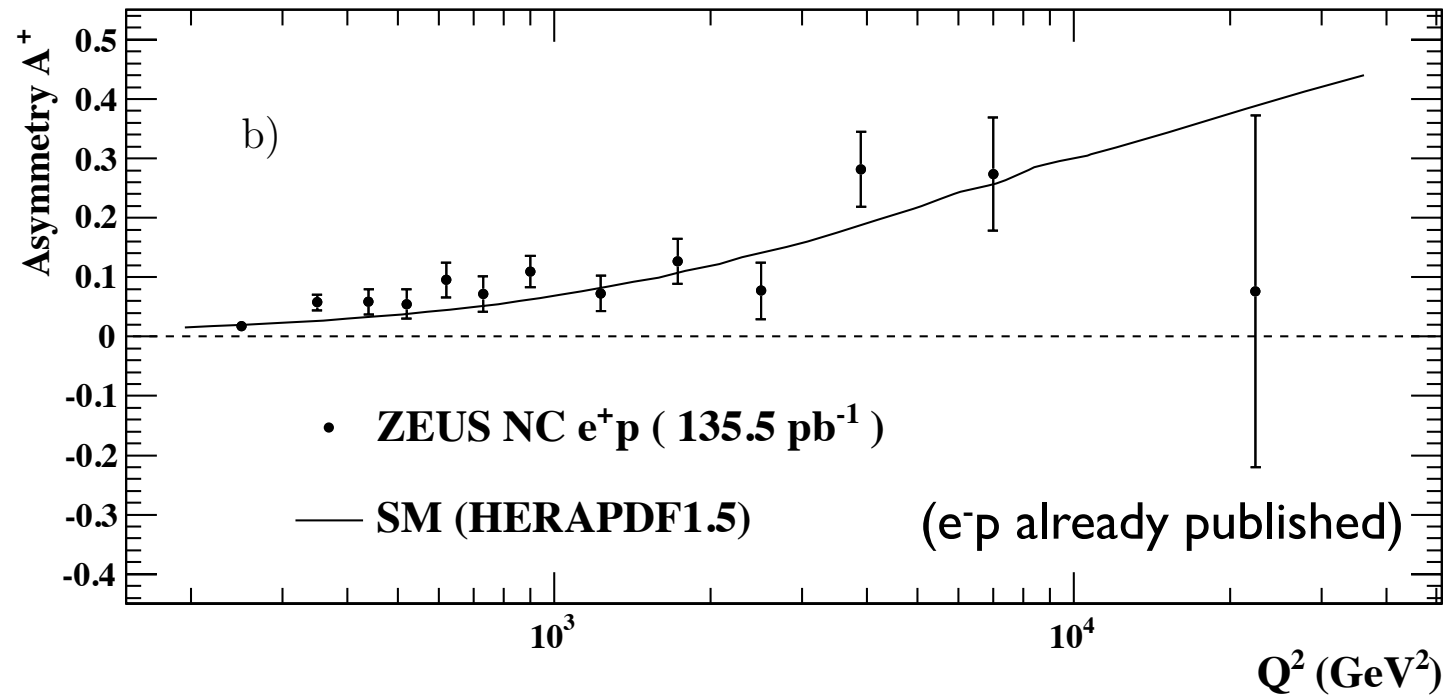
Positron scattering

$$\frac{d^2\sigma_{CC}^+}{dx dQ^2} = \frac{G_F^2}{2\pi} \left(\frac{M_W^2}{M_W^2 + Q^2} \right)^2 \left[(\bar{u} + \bar{c}) + (1 - y)^2 (d + s) \right]$$



H1 combination of high Q^2 CC data (HERA-I+II)
Improvement of total uncertainty
Dominated by statistical errors
Provide important flavour decomposition information

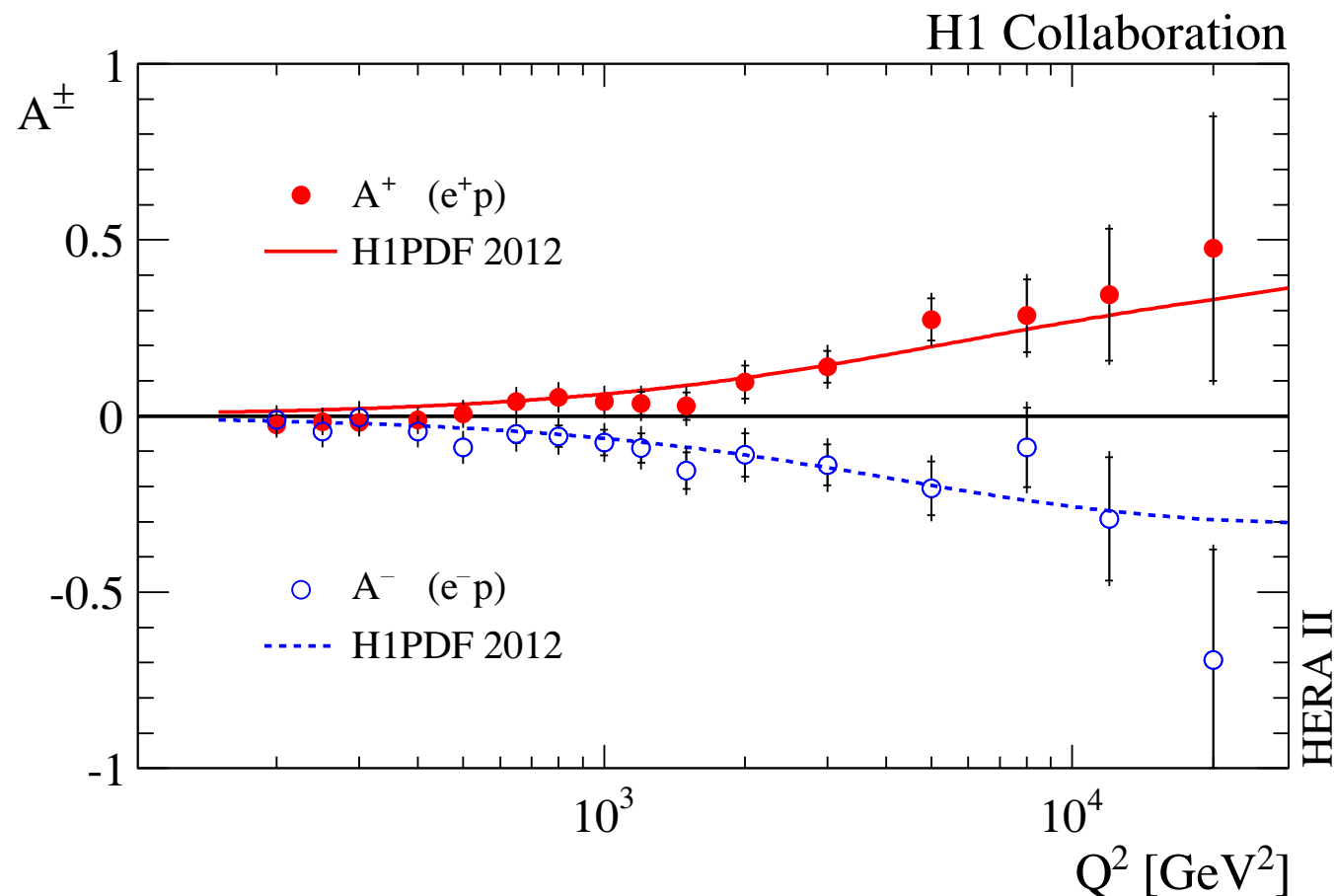
CC e^+ data provide strong d_v constraint at high x
Precision limited by statistics: typically 5-10%
HERA-I precision of 10-15% for e^+
Large gain to come after combination with ZEUS



NC polarisation asymmetry:

$$A^{\pm} = \frac{2}{P_L^{\pm} - P_R^{\pm}} \cdot \frac{\sigma^{\pm}(P_L^{\pm}) - \sigma^{\pm}(P_R^{\pm})}{\sigma^{\pm}(P_L^{\pm}) + \sigma^{\pm}(P_R^{\pm})}$$

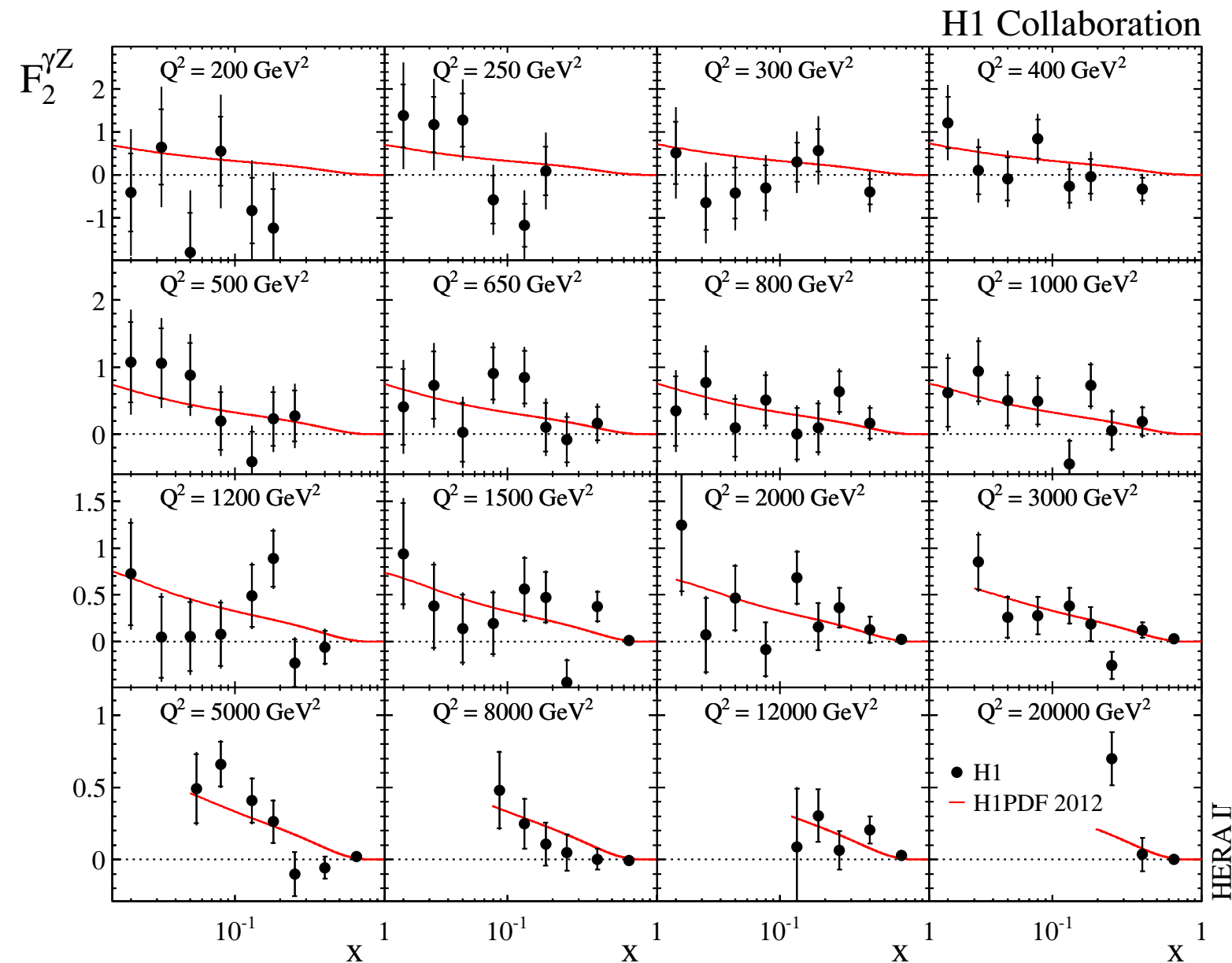
At large x $A^{\pm} \propto \pm \kappa \frac{1 + d_v/u_v}{4 + d_v/u_v}$



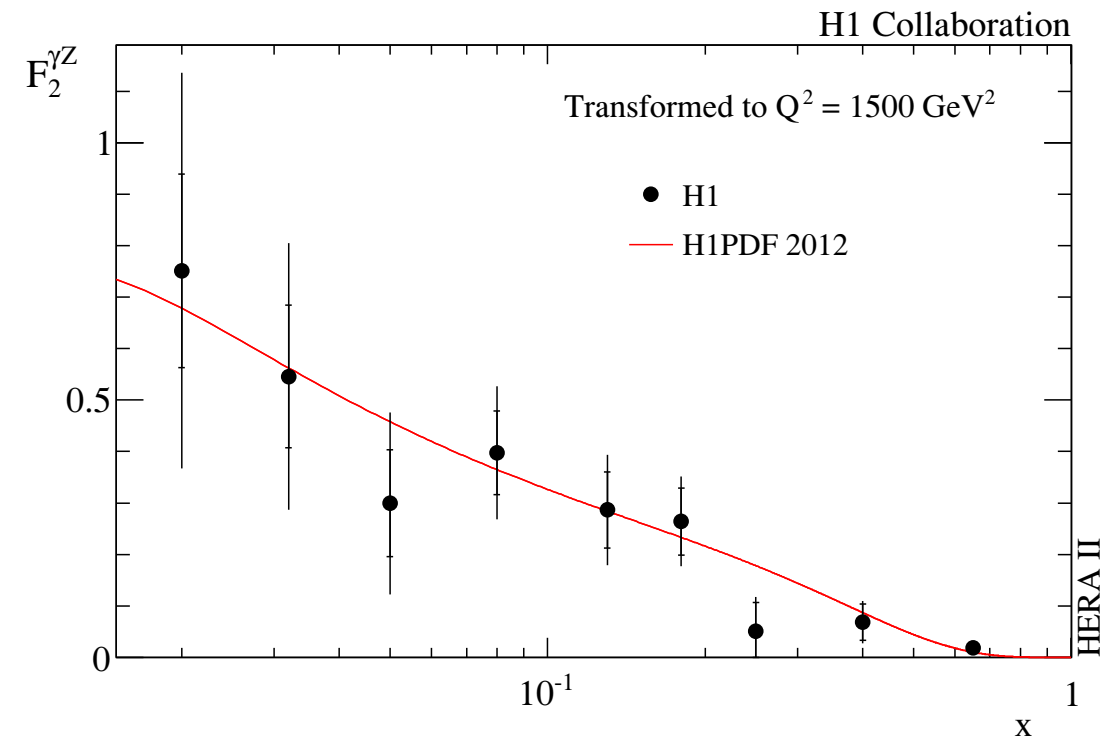
Measuring the difference in NC polarised cross sections gives access to new structure functions:

$$\frac{\sigma^\pm(P_L^\pm) - \sigma^\pm(P_R^\pm)}{P_L^\pm - P_R^\pm} = \frac{\kappa Q^2}{Q^2 + M_Z^2} \left[\boxed{\mp a_e F_2^{\gamma Z}} + \frac{Y_-}{Y_+} v_e x F_3^{\gamma Z} - \frac{Y_-}{Y_+} \frac{\kappa Q^2}{Q^2 + M_Z^2} (v_e^2 + a_e^2) x F_3^Z \right]$$

$x F_3$ terms eliminated by subtracted e^-p from e^+p



Due to different couplings $F_2^{\gamma Z}$ has different sensitivity to U-type and D-type compared to F_2



New PDF fit performed: can be thought of as a 'stepping-stone' towards HERAPDF2.0

$$xg(x) = A_g x^{B_g} (1-x)^{C_g} - A'_g x^{B'_g} (1-x)^{25},$$

$$xu_v(x) = A_{u_v} x^{B_{u_v}} (1-x)^{C_{u_v}} (1 + E_{u_v} x^2),$$

$$xd_v(x) = A_{d_v} x^{B_{d_v}} (1-x)^{C_{d_v}},$$

$$x\bar{U}(x) = A_{\bar{U}} x^{B_{\bar{U}}} (1-x)^{C_{\bar{U}}},$$

$$x\bar{D}(x) = A_{\bar{D}} x^{B_{\bar{D}}} (1-x)^{C_{\bar{D}}}.$$

| Parameter | Central Value | Lower Limit | Upper Limit |
|----------------------------------|---------------|------------------------------|---------------------------------|
| f_s | 0.31 | 0.23 | 0.38 |
| m_c (GeV) | 1.4 | 1.35 (for $Q_0^2 = 1.8$ GeV) | 1.65 |
| m_b (GeV) | 4.75 | 4.3 | 5.0 |
| Q_{\min}^2 (GeV ²) | 3.5 | 2.5 | 5.0 |
| Q_0^2 (GeV ²) | 1.9 | 1.5 ($f_s = 0.29$) | 2.5 ($m_c = 1.6, f_s = 0.34$) |

13 parameter fit: additional flexibility given to u_v and d_v compared to H1PDF2009 / HERAPDF1.0

Apply momentum/counting sum rules:

$$\int_0^1 dx \cdot (xu_v + xd_v + x\bar{U} + x\bar{D} + xg) = 1$$

$$\int_0^1 dx \cdot u_v = 2 \quad \int_0^1 dx \cdot d_v = 1$$

Parameter constraints:

$$B_{\text{Ubar}} = B_{\text{Dbar}}$$

$$\text{sea} = 2 \times (\text{Ubar} + \text{Dbar})$$

$$\text{Ubar} = \text{Dbar at } x=0$$

$$f_s = \text{sbar/Dbar}$$

$$Q_0^2 = 1.9 \text{ GeV}^2 \text{ (below } m_c)$$

$$Q^2 > 3.5 \text{ GeV}^2$$

$$2 \times 10^{-4} < x < 0.65$$

Fits performed using RT-VFNS

Experimental uncertainties produced using RMS spread of 400 replica fits

Parameterisation uncertainty determined from envelope of 14 parameter fit & Q_0^2 variations

Error band is applied to central value fit \Rightarrow asymmetric errors since mean of replicas \neq central fit

$$\chi^2 = \sum_i \frac{\left[\mu_i - m_i \left(1 - \sum_j \gamma_j^i b_j \right) \right]^2}{\delta_{i,\text{unc}}^2 m_i^2 + \delta_{i,\text{stat}}^2 \mu_i m_i \left(1 - \sum_j \gamma_j^i b_j \right)} + \sum_j b_j^2 + \sum_i \ln \frac{\delta_{i,\text{unc}}^2 m_i^2 + \delta_{i,\text{stat}}^2 \mu_i m_i}{\delta_{i,\text{unc}}^2 \mu_i^2 + \delta_{i,\text{stat}}^2 \mu_i^2}$$

μ_i measurement i

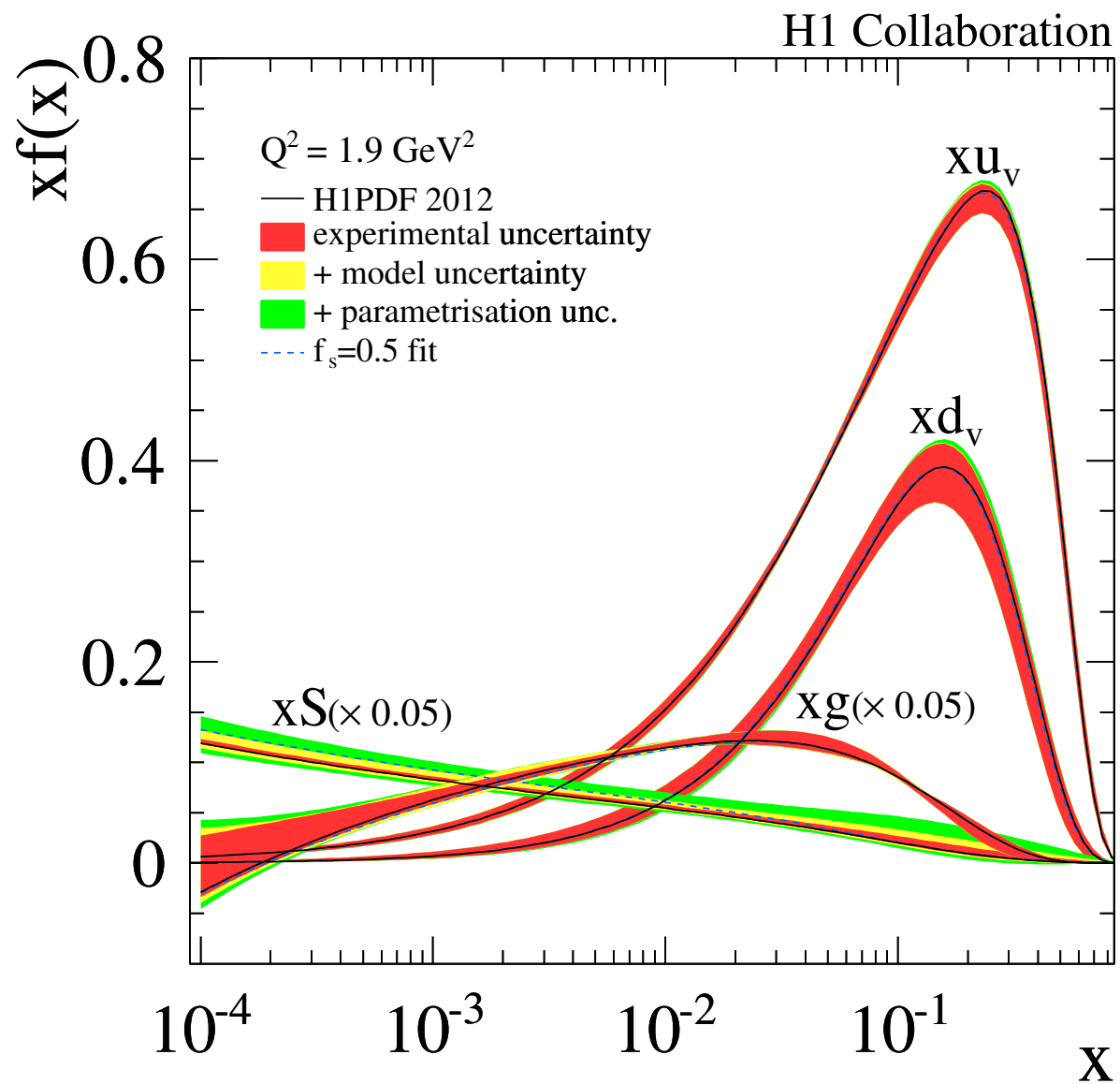
m_i theory i

b_j correlated sys source j

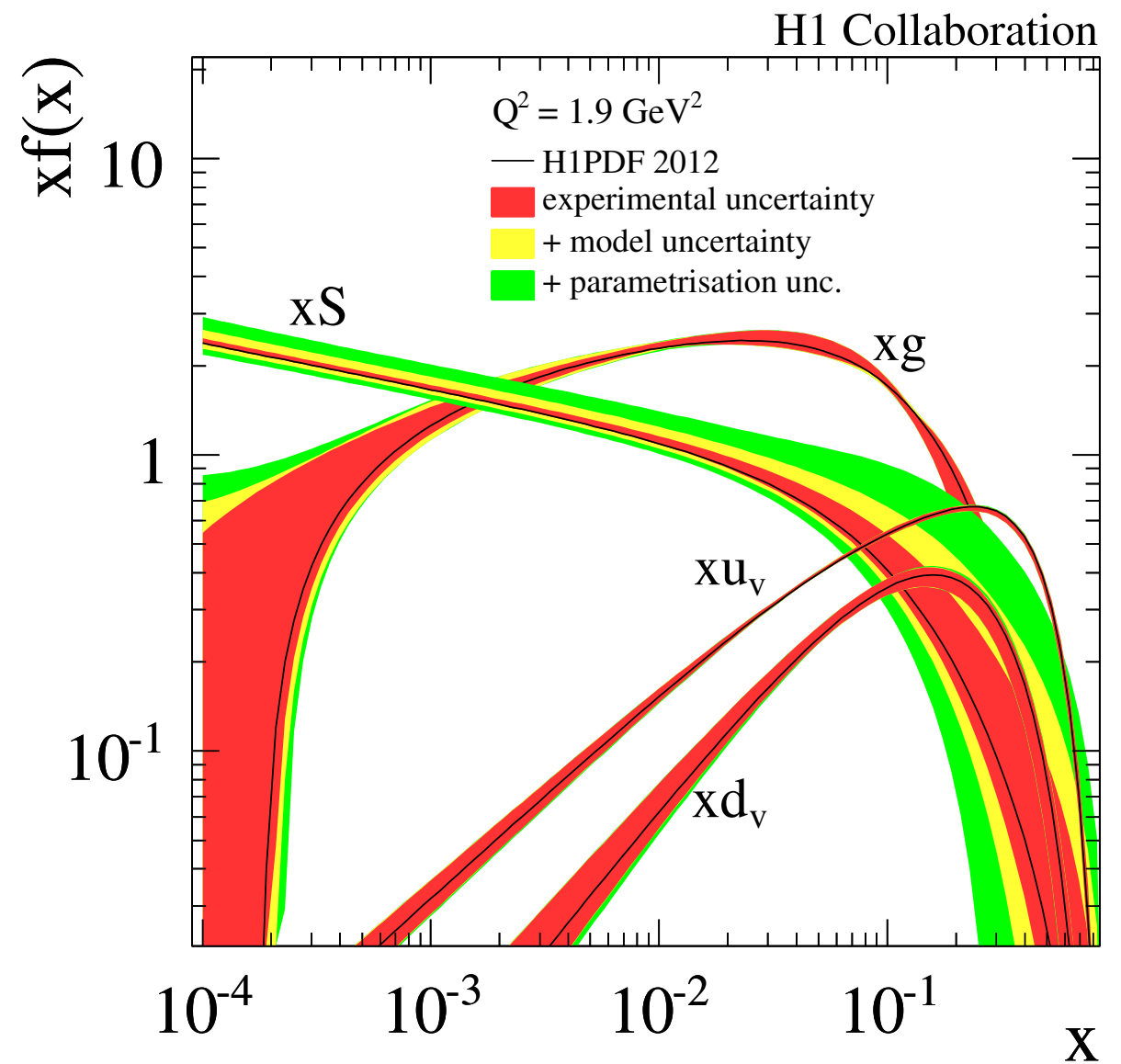
γ_j^i correlated error i,j

Errors prop to measured values - avoid stat fluctuations by scaling errors by expectation m_i

Modified χ^2 definition includes \ln term to account for likelihood transition to χ^2 after error scaling



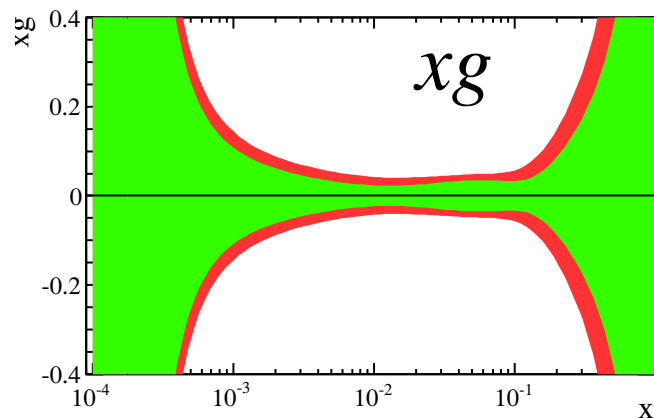
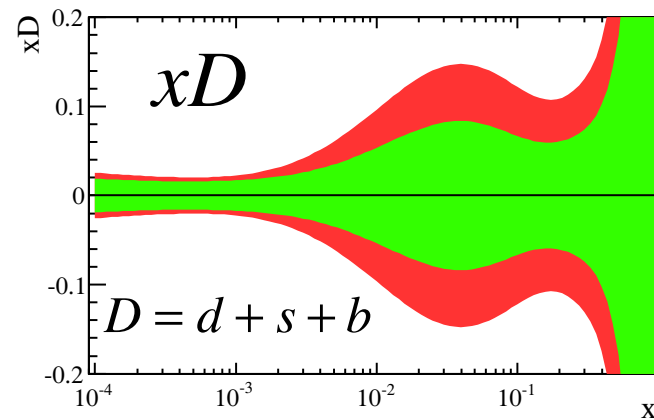
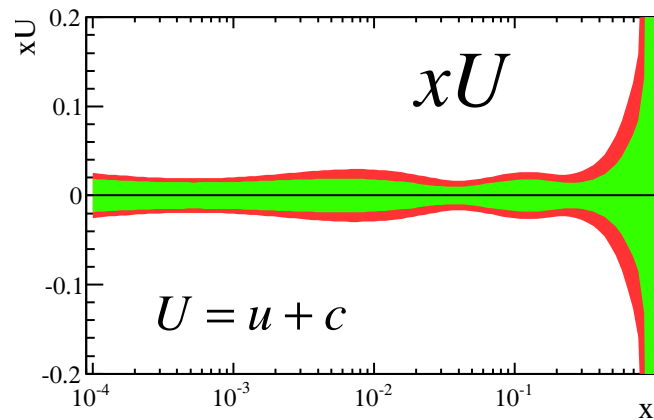
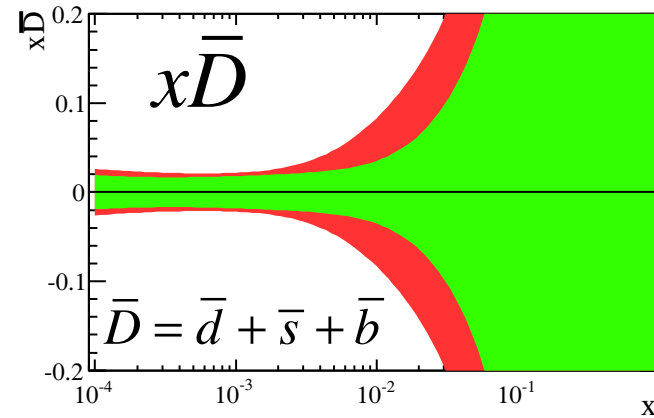
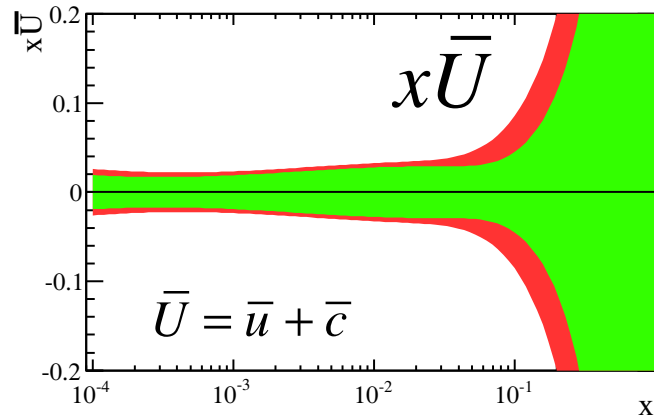
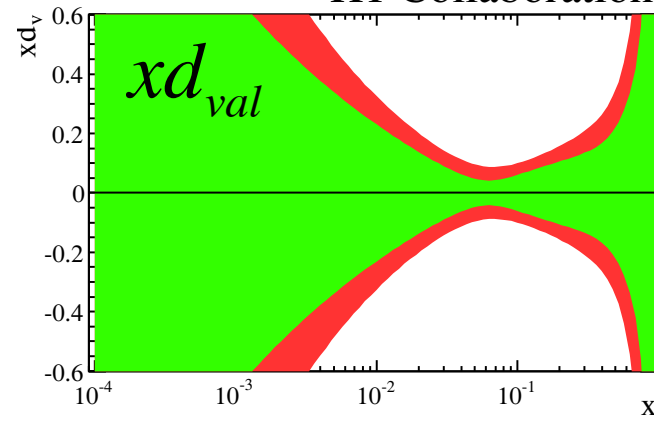
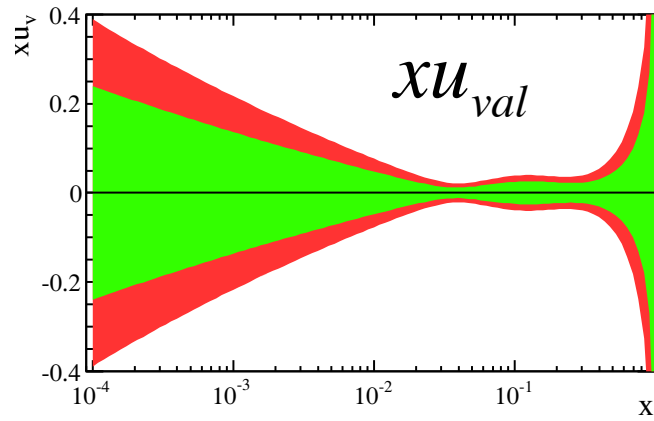
$$\chi^2/\text{ndf} = 1570/1461 = 1.07$$



Fit with unsuppressed strange sea ($f_s=0.5$) is well within error bands

PDF Uncertainties

H1 Collaboration



Uncert. due to H1 HERA I data

Uncert. due to H1 HERA I+II data

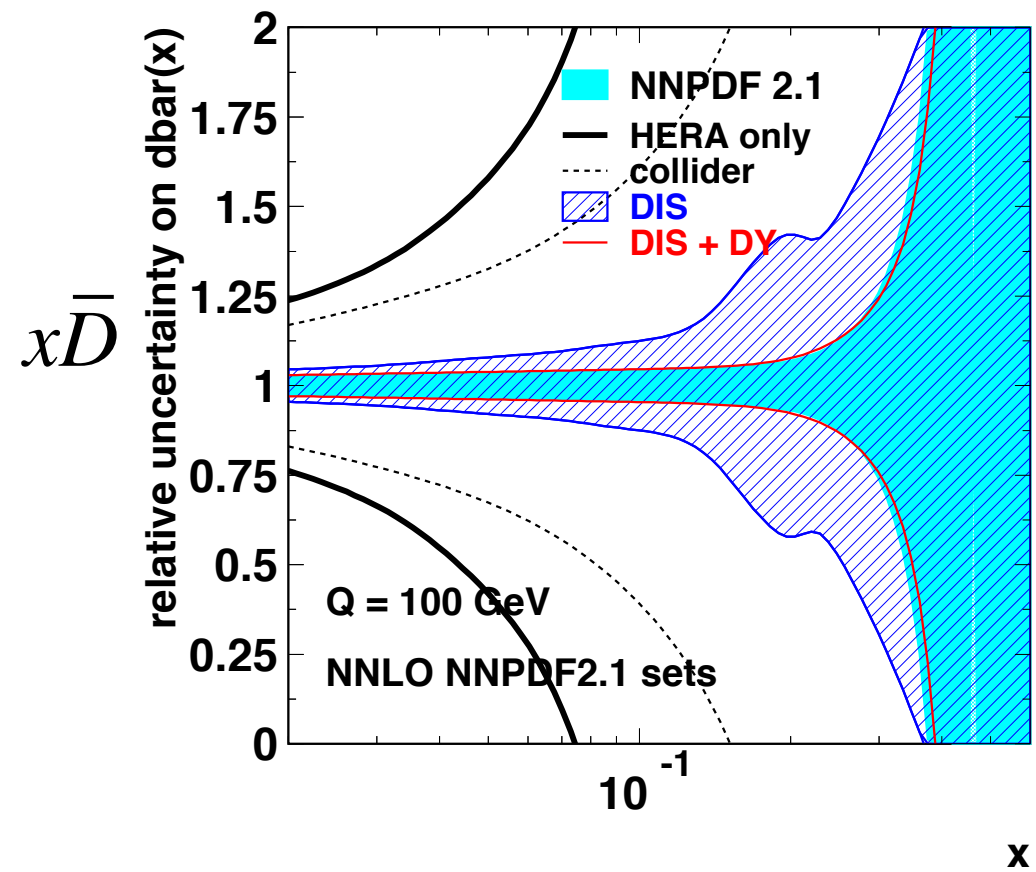
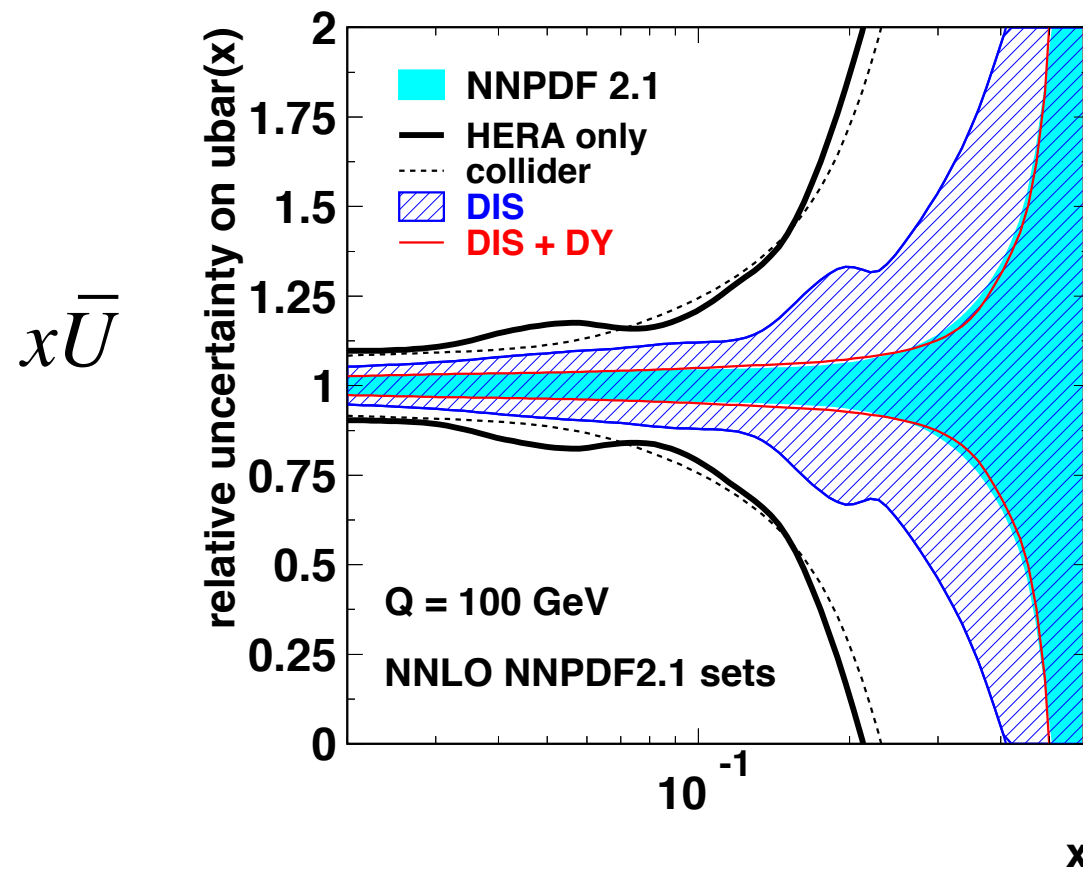
$$Q^2 = 1.9 \text{ GeV}^2$$

Comparison of PDF uncertainties from H1 fits with and without new HERA-II data

Large improvement in xd_v and xD over wide x range - driven by more precise CC e^+p data

Improvement in xu_v from NC at high x . Error reduction at low x arises from sum rules

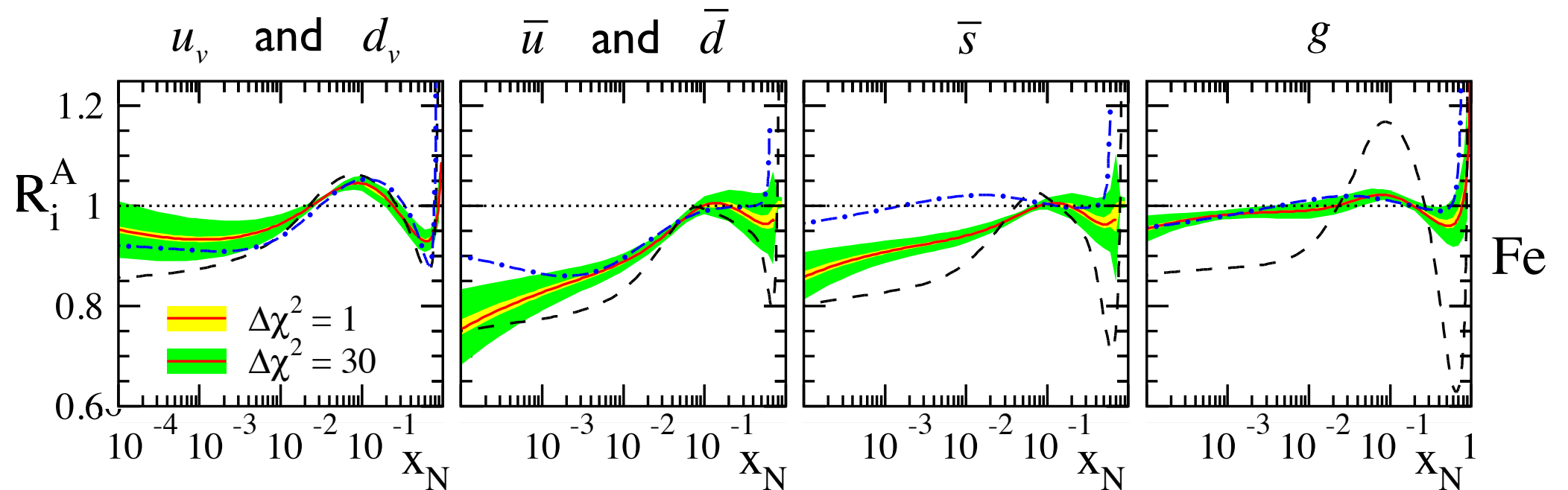
High x gluon is also improved from scaling violations



HERA-I data only

At high x strongest constraints on anti-quarks from deuterium Drell-Yan measurements
Also d quark constraints from deuterium DIS

Cross section ratio
for Fe : proton target



HERAPDF philosophy: Fewer data sets \rightarrow better control of experimental uncertainties
PDF experimental uncertainty defined by $\Delta\chi^2=1$ criterion
Compare to MSTW / CTEQ: effectively use $\Delta\chi^2=50$ to 100
Avoid complications of data using nuclear targets

HERAPDF2.0

Include final:

HERA-I low/medium Q^2 precision F_2

HERA-II high Q^2 polarised NC/CC data

HERA-II low/medium $E_p=575/460$ GeV energy NC data

HERA-I+II F_2^{cc} combined data - almost ready

HERA-I+II multijet data - awaiting H1 publication

Expect several fits:

NLO vs NNLO

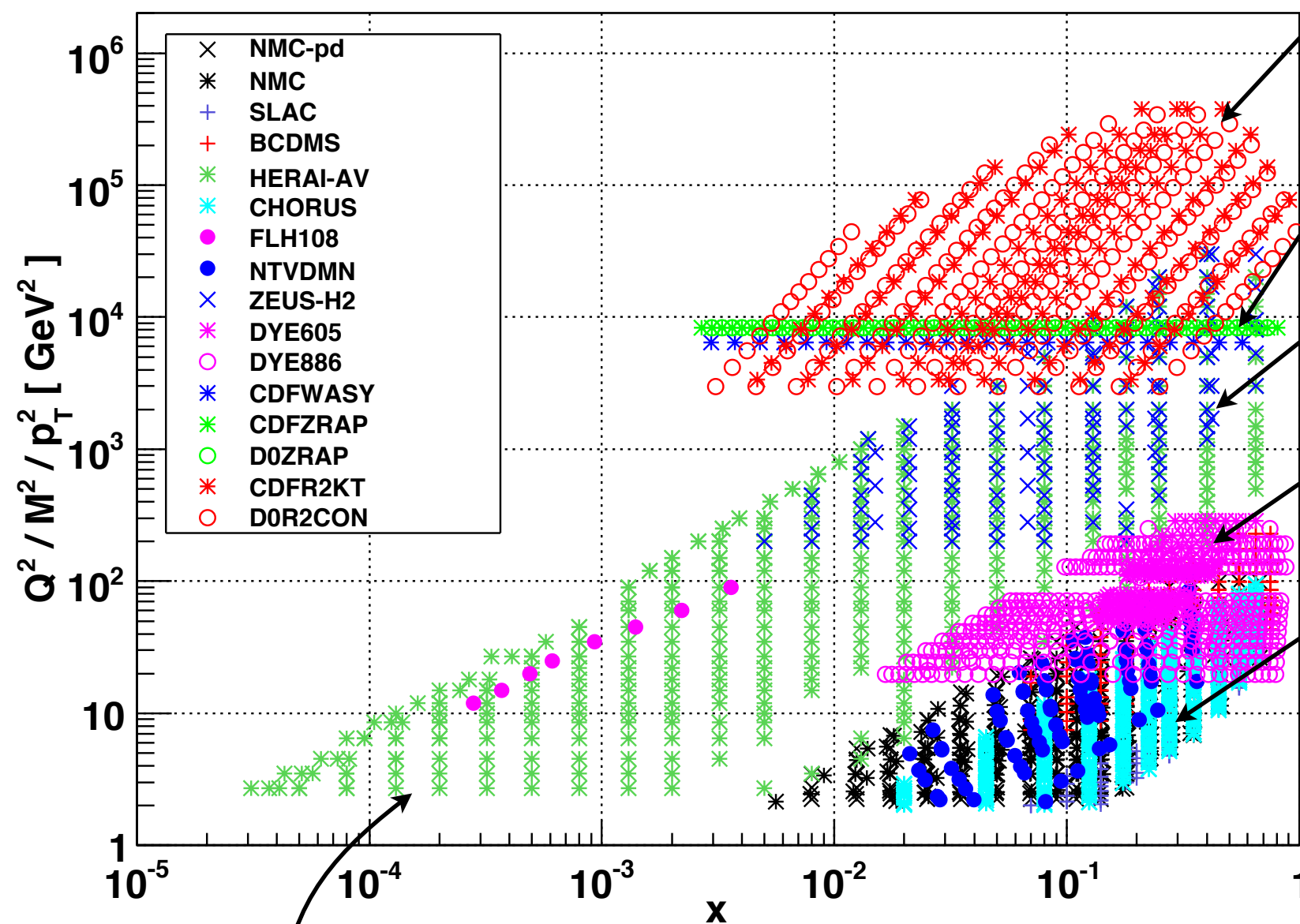
NLO will be: inclusive NC/CC data & inclusive + F_2^{cc} (+ jets?)

Include fit to α_s

MC method for experimental errors will be used

Timescale \sim spring 2013 (DIS workshop?)

Typical datasets used in global PDF analyses



HERA-I data

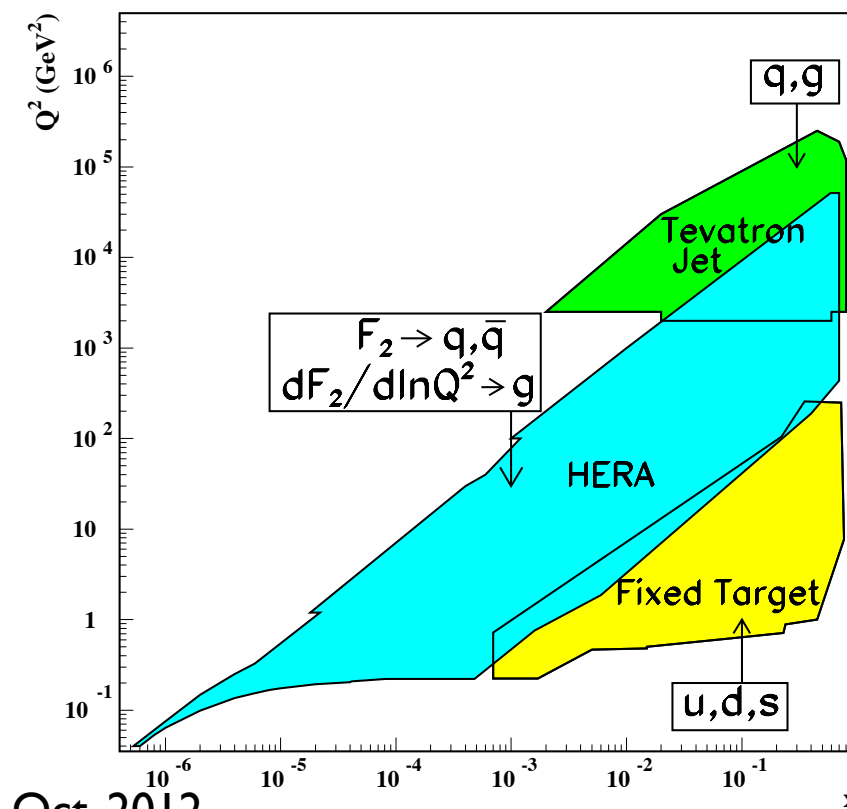
Tevatron jets

Tevatron W asymmetry
Tevatron Z rapidity

HERA-II high Q^2 data

Drell-Yan fixed target
E605 / E772 / E886

DIS fixed target
NMC / BCDMS



W^\pm lepton charge asymmetry

$$A(\eta) = \frac{d\sigma/d\eta(W^+ \rightarrow l^+ \nu) - d\sigma/d\eta(W^- \rightarrow l^- \bar{\nu})}{d\sigma/d\eta(W^+ \rightarrow l^+ \nu) + d\sigma/d\eta(W^- \rightarrow l^- \bar{\nu})}$$

$$W^+ : u\bar{d} + c\bar{s}$$

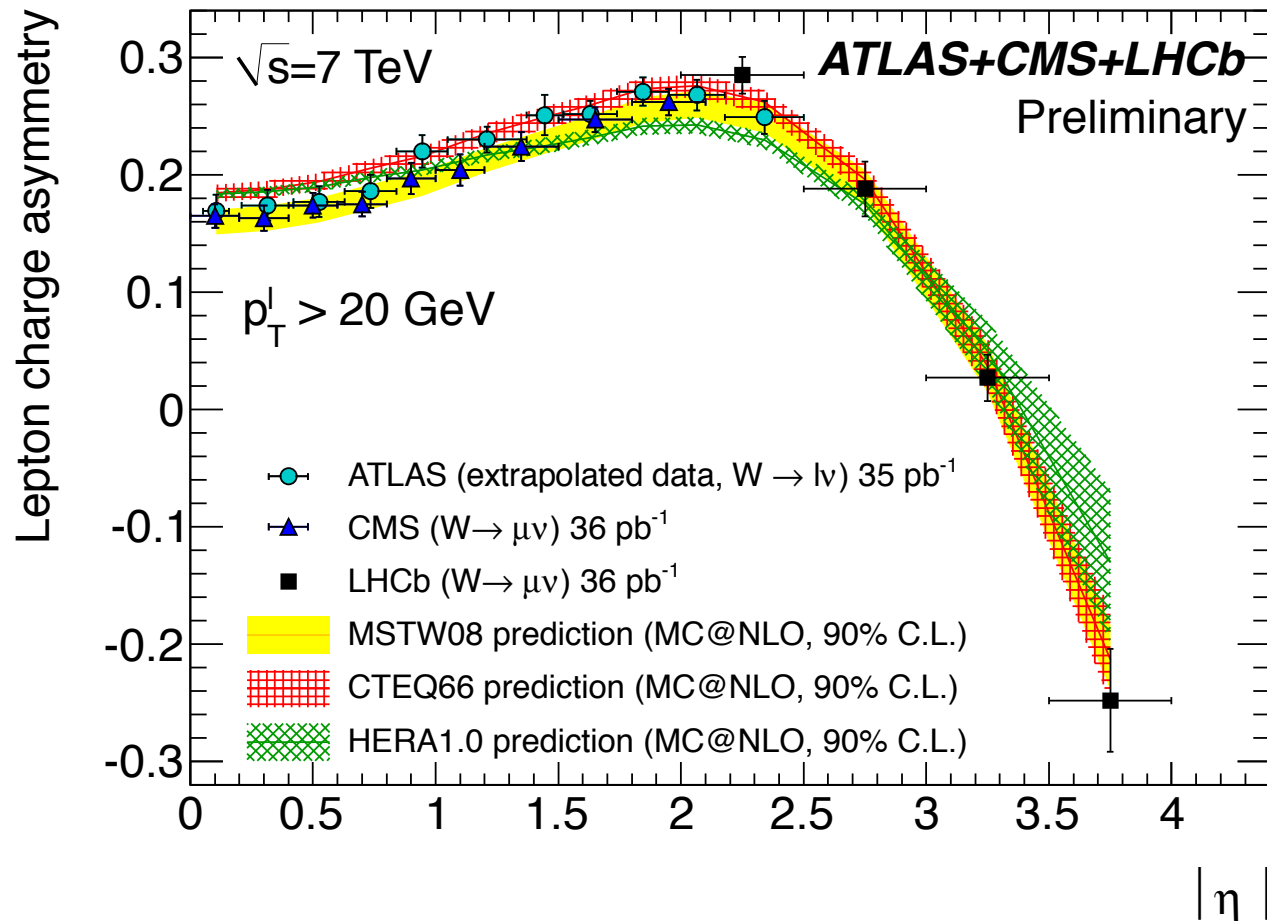
$$W^- : d\bar{u} + s\bar{c}$$

probes flavour structure

D0 measurements show tension with CDF

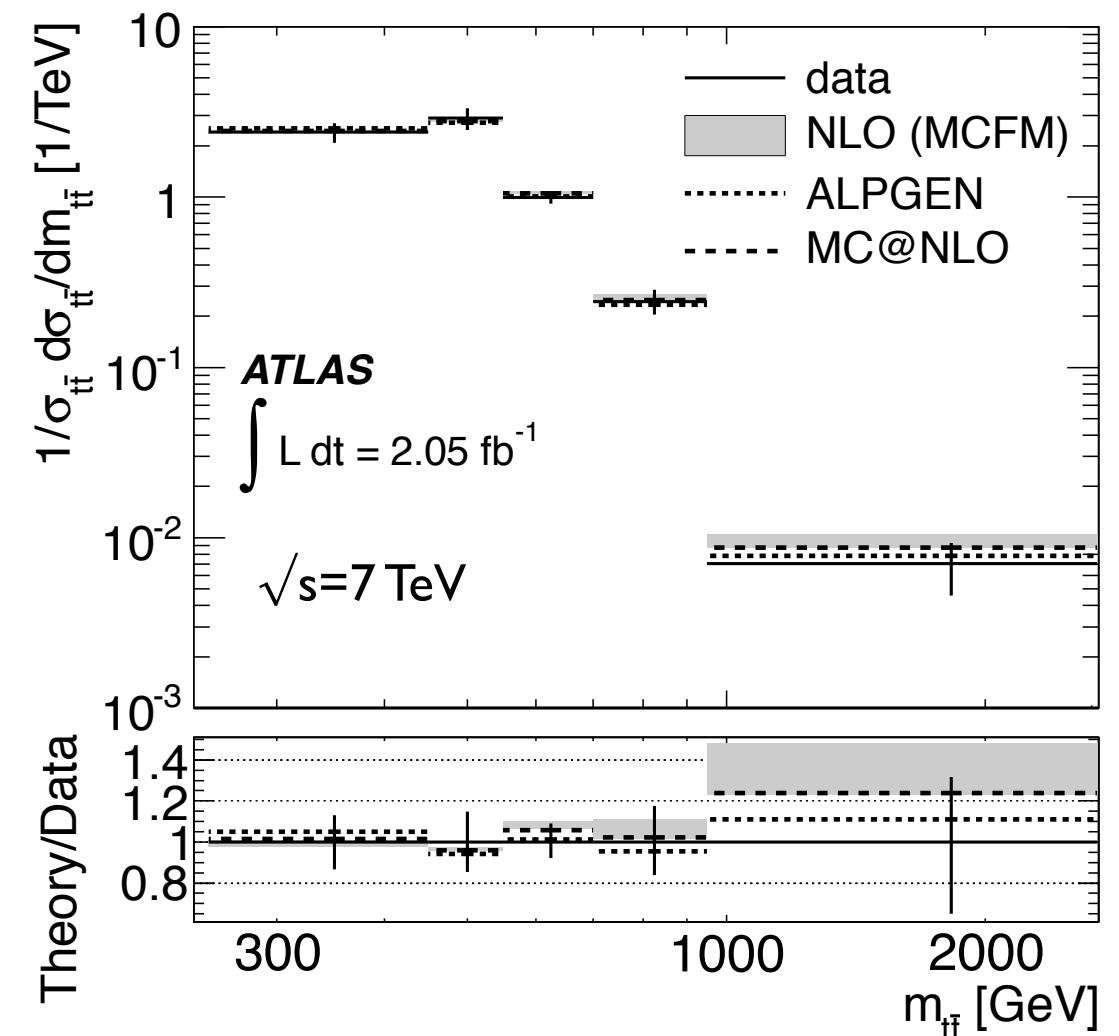
Alleviated with improved flexibility of PDF functions?

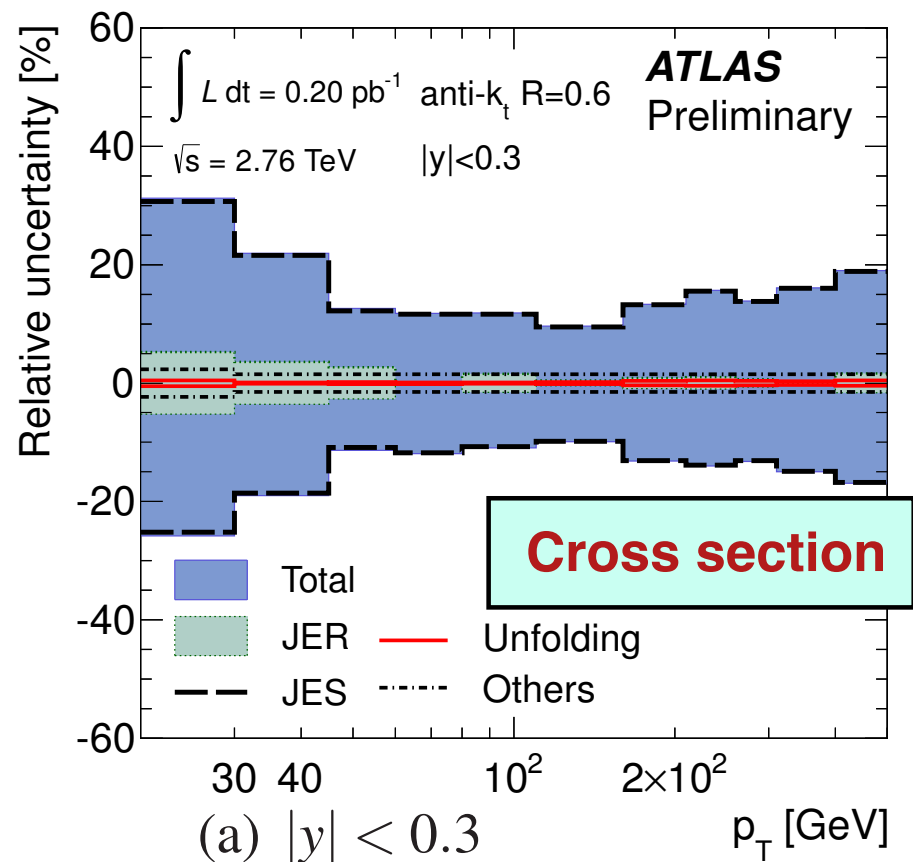
(Thorne, PDF4LHC Workshop, Sept 2012)



Top/anti-top differential cross section

At $\sqrt{s}=14$ TeV dominant contribution 90% is from gg
Constrains high x gluon





LHC inclusive jets

Can reach very high $x \sim 0.9$

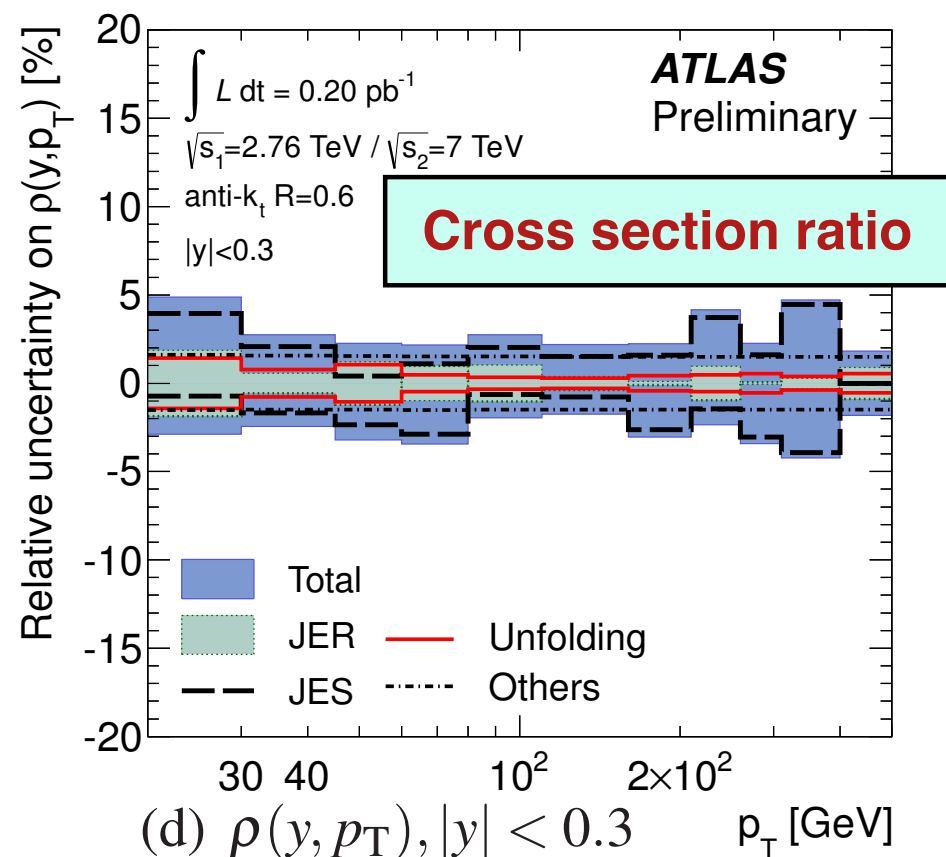
Constrains qq and qg at high x

Large detector uncertainty from energy scale

Reduce error by taking cross section ratio at different \sqrt{s}

\Rightarrow correlated systematic errors \sim cancel

Atlas published data for $\sqrt{s}=2.76 \text{ TeV}$ and $\sqrt{s}=7 \text{ TeV}$



Other LHC constraints

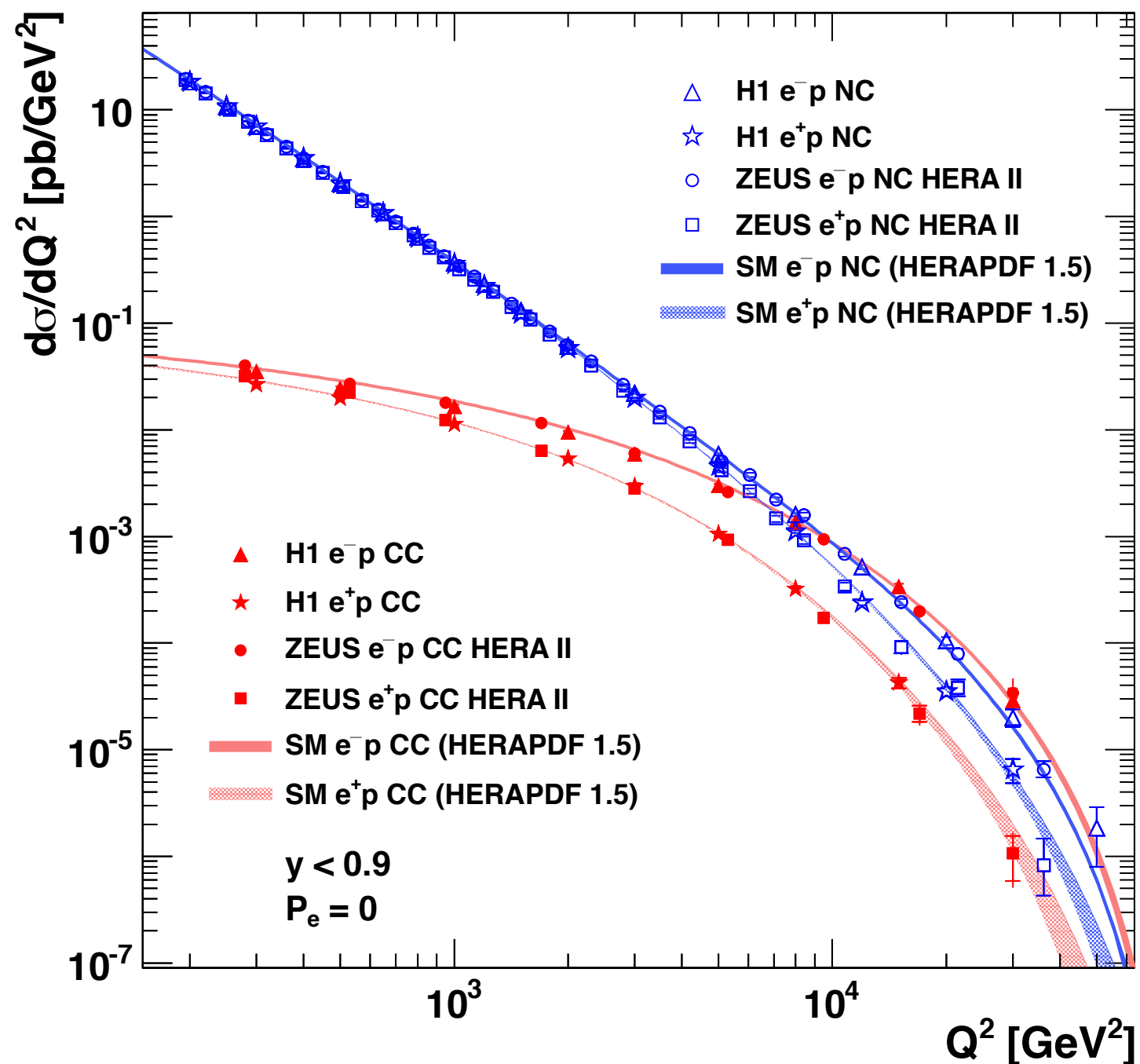
$W^+ + c$ & $W^- + c$ gives access to strange/anti-strange

High mass Drell-Yan \rightarrow anti-quarks at high x

Prompt photon production $qg \rightarrow \gamma q$ constrains high x gluon

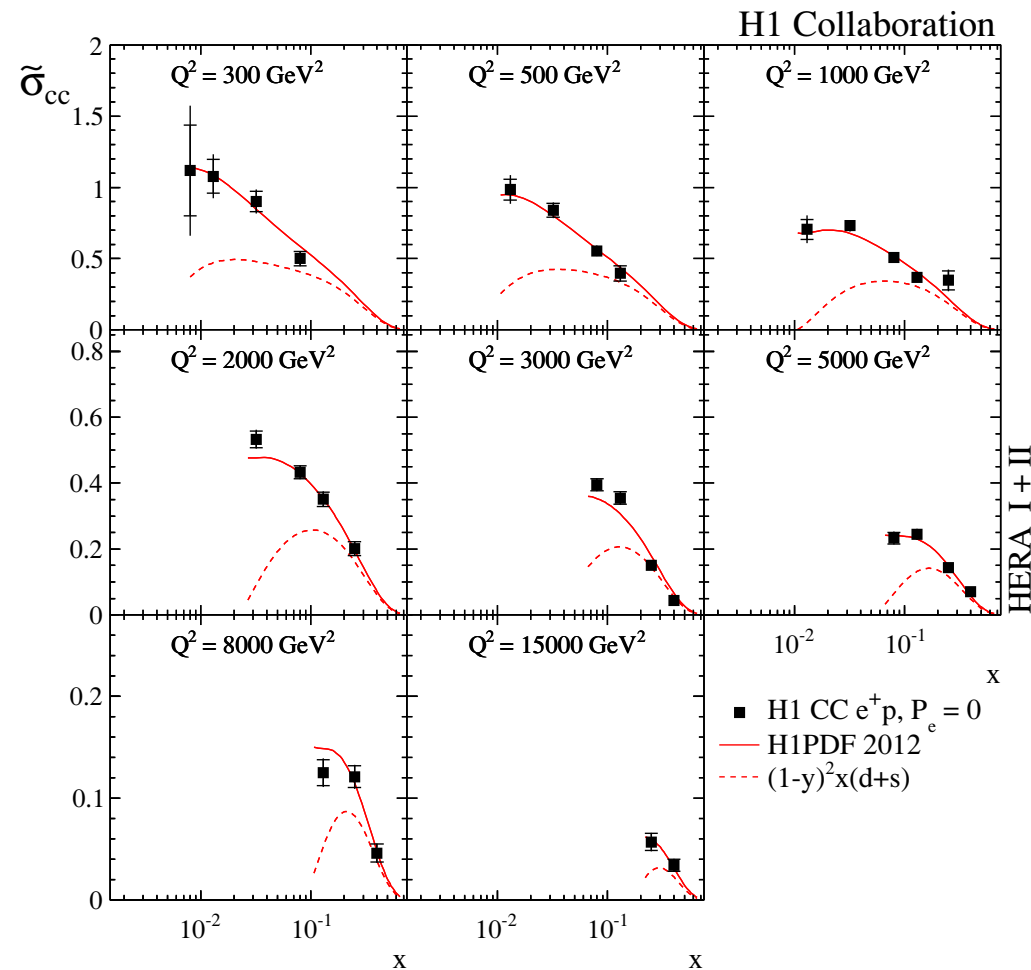
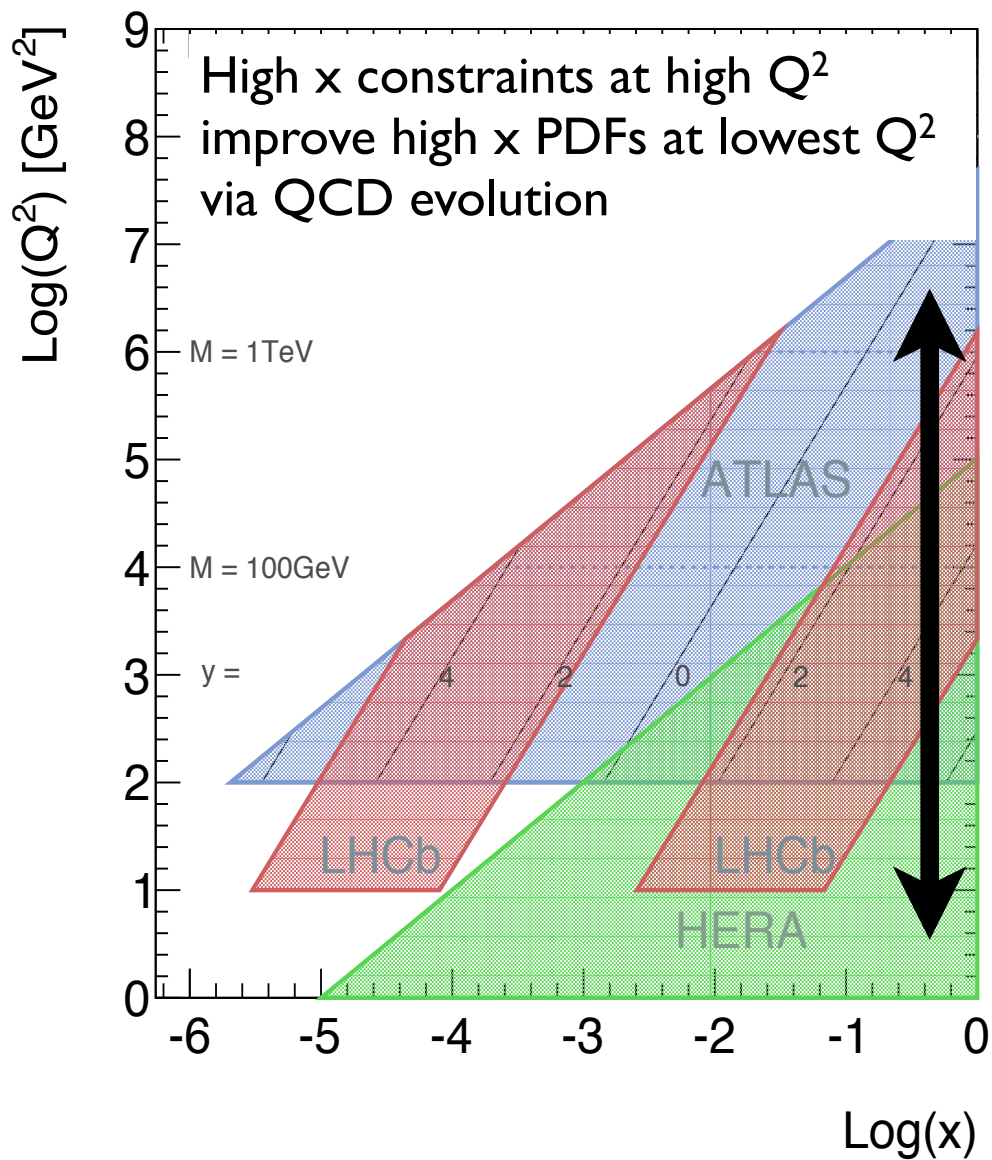
....

HERA



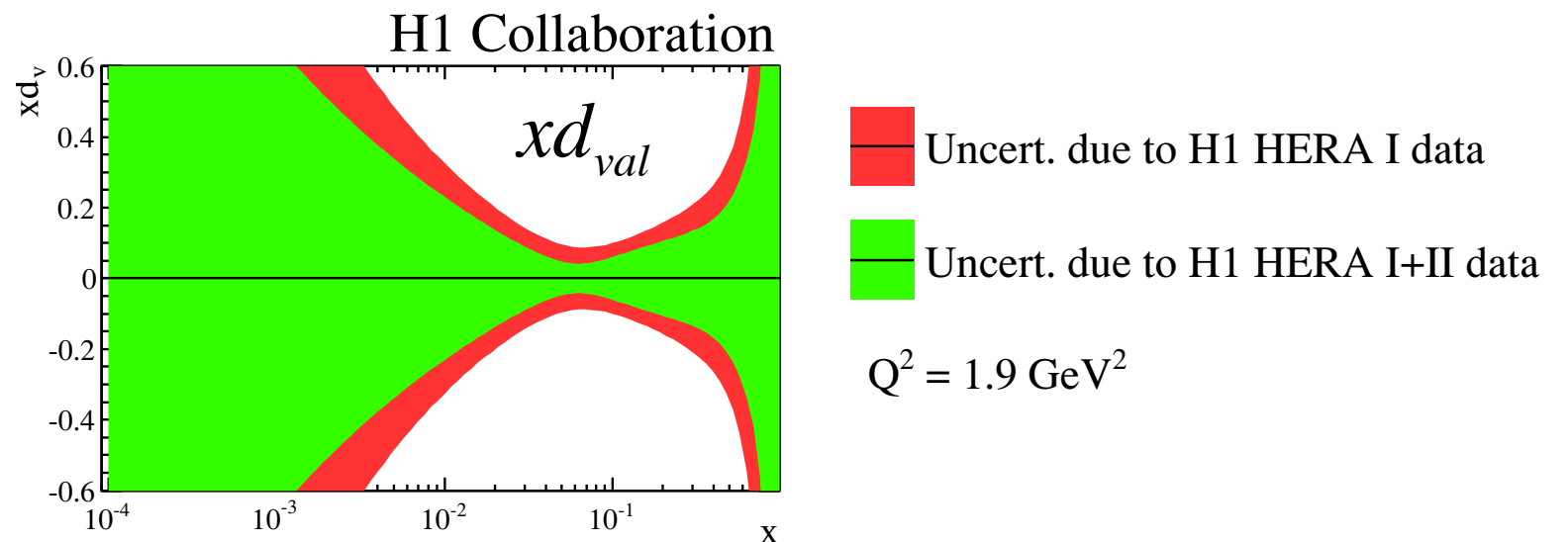
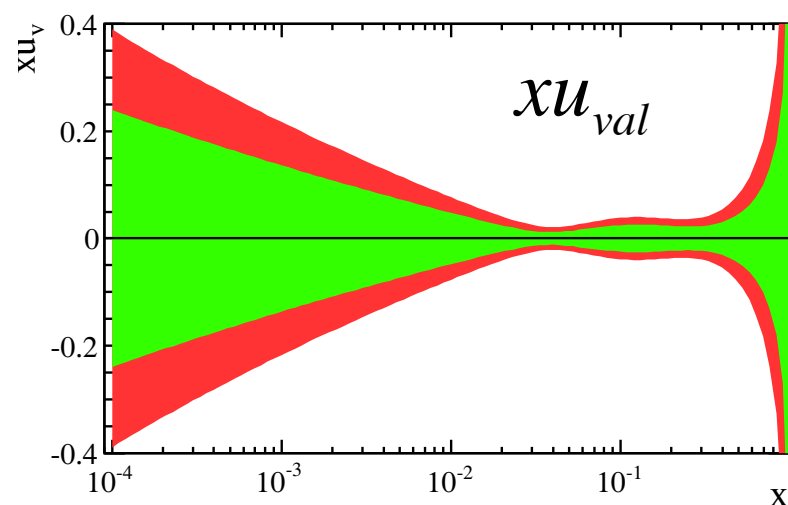
- H1 / ZEUS completed their final SF measurements
- New HERA-II data provide tighter constraints at high x / Q^2
- HERA data provide some of the most stringent constraints on PDFs
- Stress-test of QCD over 4 orders of mag. in Q^2
- DGLAP evolution works very well
- HERA data provide a self-consistent data set for complete flavour decomposition of the proton
- New combination of HERA data underway
- Combination \Rightarrow HERAPDF2.0 QCD fit
- Global PDF analyses now start to use LHC data



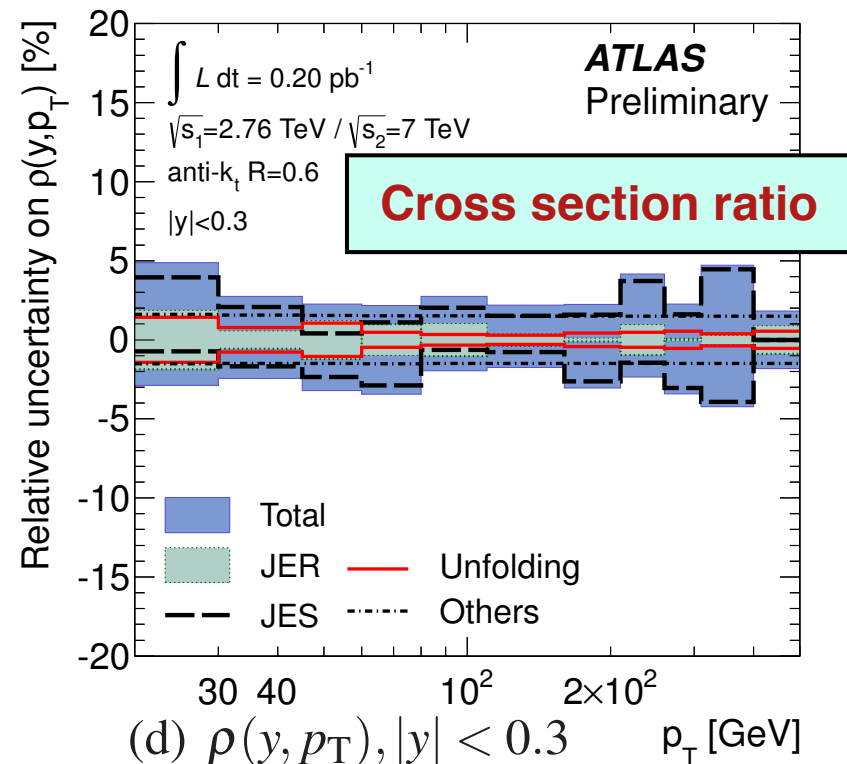
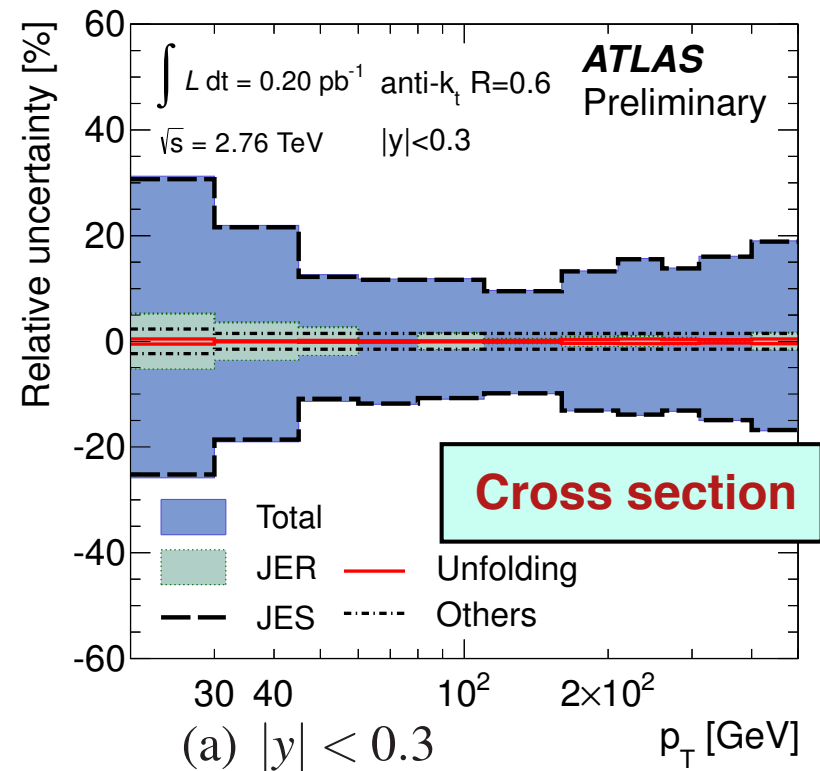


Final high x / high Q^2 NC and CC cross sections now published from H1 & ZEUS - legacy data sets

CC e^+p gives strong clean constraints on $x d_v$



Inclusive jets at $\sqrt{s}=2.76$ TeV and $\sqrt{s}=7$ TeV
Constrain qg and gg PDFs



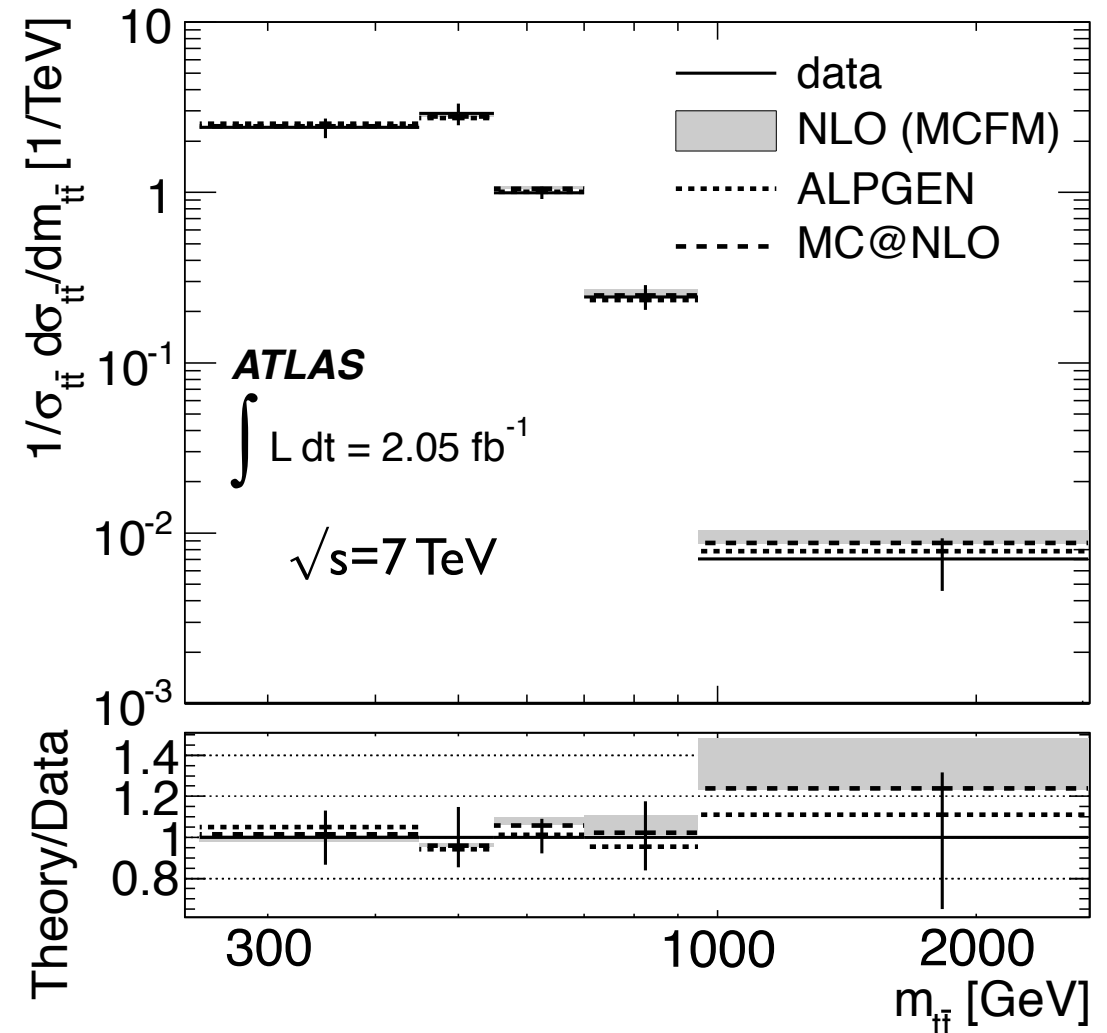
LHC data provide new high x constraints
Yet to be included in QCD fits to PDFs

← two examples ↓

Top/anti-top differential cross section

First measurement at $\sqrt{s}=7$ TeV

Large stat error - future $\sqrt{s}=14$ TeV will give better constraints

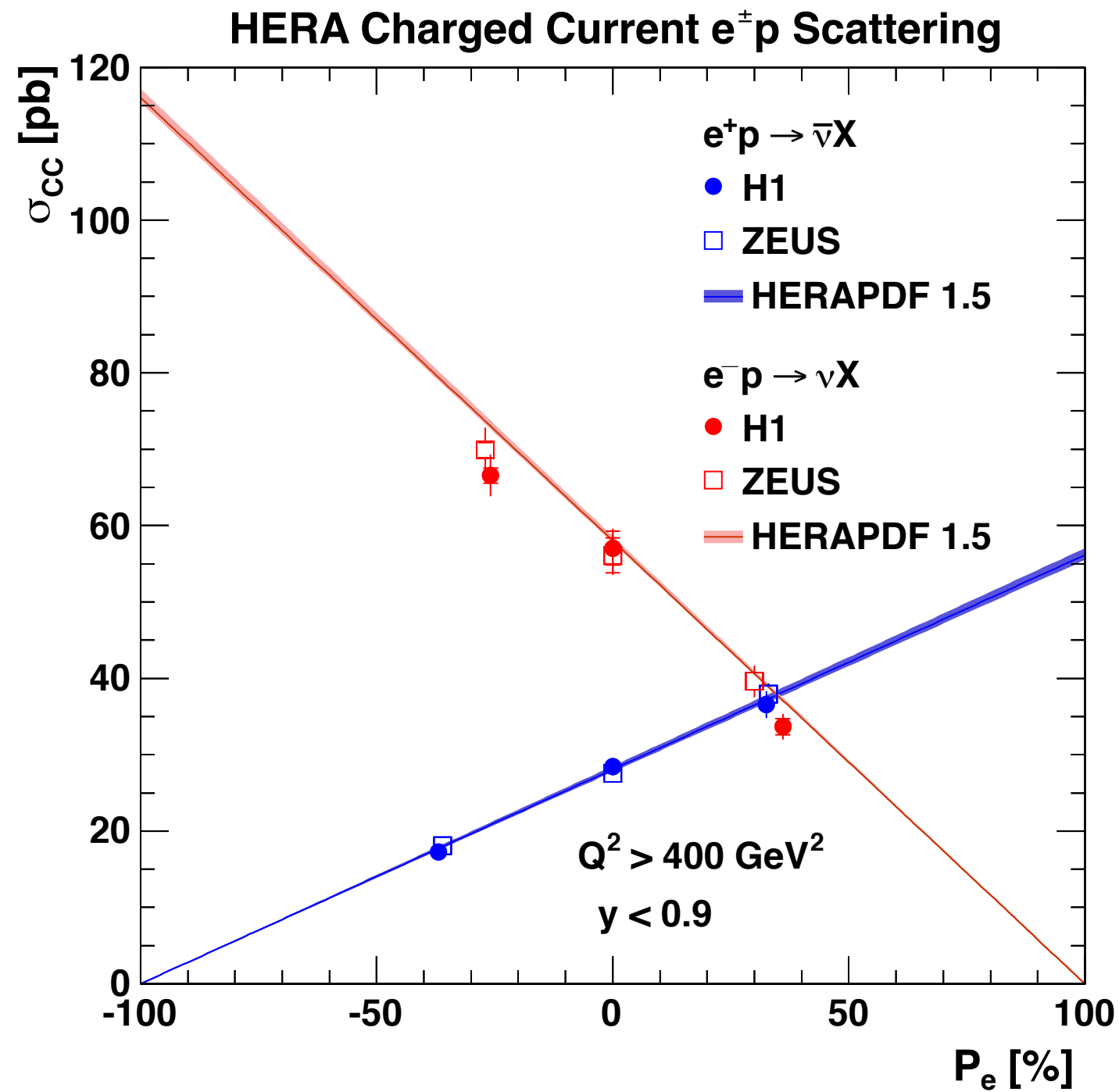


Summary of HERA-I datasets Combined in HERAPDF1.0

Available since 2009

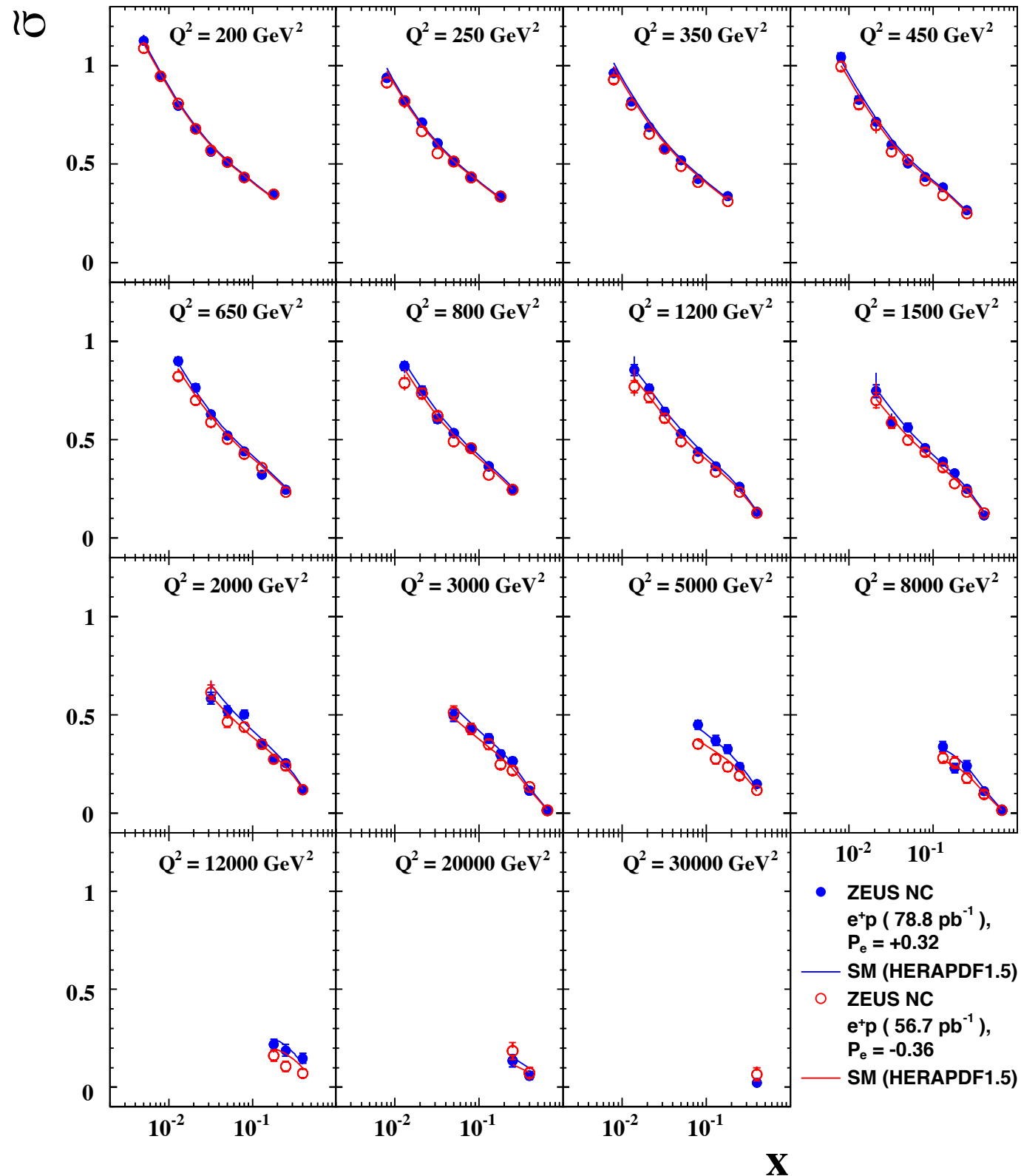
| Data Set | | x Range | | Q^2 Range GeV ² | | \mathcal{L} pb ⁻¹ | e^+/e^- | \sqrt{s} GeV |
|--------------|-------|----------------------|--------------------|---------------------------------|-------|-----------------------------------|-----------|-------------------|
| H1 svx-mb | 95-00 | 5×10^{-6} | 0.02 | 0.2 | 12 | 2.1 | e^+p | 301-319 |
| H1 low Q^2 | 96-00 | 2×10^{-4} | 0.1 | 12 | 150 | 22 | e^+p | 301-319 |
| H1 NC | 94-97 | 0.0032 | 0.65 | 150 | 30000 | 35.6 | e^+p | 301 |
| H1 CC | 94-97 | 0.013 | 0.40 | 300 | 15000 | 35.6 | e^+p | 301 |
| H1 NC | 98-99 | 0.0032 | 0.65 | 150 | 30000 | 16.4 | e^-p | 319 |
| H1 CC | 98-99 | 0.013 | 0.40 | 300 | 15000 | 16.4 | e^-p | 319 |
| H1 NC HY | 98-99 | 0.0013 | 0.01 | 100 | 800 | 16.4 | e^-p | 319 |
| H1 NC | 99-00 | 0.0013 | 0.65 | 100 | 30000 | 65.2 | e^+p | 319 |
| H1 CC | 99-00 | 0.013 | 0.40 | 300 | 15000 | 65.2 | e^+p | 319 |
| ZEUS BPC | 95 | 2×10^{-6} | 6×10^{-5} | 0.11 | 0.65 | 1.65 | e^+p | 301 |
| ZEUS BPT | 97 | 6×10^{-7} | 0.001 | 0.045 | 0.65 | 3.9 | e^+p | 301 |
| ZEUS SVX | 95 | 1.2×10^{-5} | 0.0019 | 0.6 | 17 | 0.2 | e^+p | 301 |
| ZEUS NC | 96-97 | 6×10^{-5} | 0.65 | 2.7 | 30000 | 30.0 | e^+p | 301 |
| ZEUS CC | 94-97 | 0.015 | 0.42 | 280 | 17000 | 47.7 | e^+p | 301 |
| ZEUS NC | 98-99 | 0.005 | 0.65 | 200 | 30000 | 15.9 | e^-p | 319 |
| ZEUS CC | 98-99 | 0.015 | 0.42 | 280 | 30000 | 16.4 | e^-p | 319 |
| ZEUS NC | 99-00 | 0.005 | 0.65 | 200 | 30000 | 63.2 | e^+p | 319 |
| ZEUS CC | 99-00 | 0.008 | 0.42 | 280 | 17000 | 60.9 | e^+p | 319 |

High Q^2 NC and CC data limited to
100 pb⁻¹ e^+p
16 pb⁻¹ e^-p



Polarisation dependence of CC cross section
 now final from H1 and ZEUS

ZEUS



Polarised NC measurements completed
for e^+p , e^-p , L-handed , R-handed scattering

Difference in L,R scattering visible at high Q^2

HERAPDF1.0

Combine NC and CC HERA-I data from H1 & ZEUS

Complete MSbar NLO fit

NLO: standard parameterisation with 10 parameters

$\alpha_s = 0.1176$ (fixed in fit)

HERAPDF1.5

Include additional NC and CC HERA-II data

Complete MSbar NLO and NNLO fit

NLO: standard parameterisation with 10 parameters

HERAPDF1.5f

NNLO: extended fit with 14 parameters

HERAPDF1.6

Include additional NC inclusive jet data $5 < Q^2 < 15000$

Complete MSbar NLO fit

NLO: standard parameterisation with 14 parameters

$\alpha_s = 0.1202 \pm 0.0013$ (exp) ± 0.004 (scales) free in fit

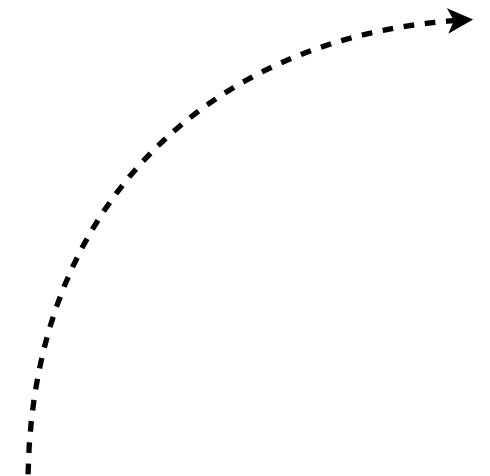
HERAPDF1.7

Include 41 additional F_2^{cc} data $4 < Q^2 < 1000$

Include 224 combined cross section points $E_p=575/460$ GeV

Complete MSbar NLO fit

NLO: standard parameterisation with 14 parameters



New H1 data are combined with all previously published H1 inclusive cross section measurements

854 data points averaged to 413 measurements

$$\chi^2/\text{ndf} = 412/441 = 0.93$$

Normalisation shifts for H1 data after averaging

| Source | Shift in units of standard deviation | Shift in % of cross section |
|--|--------------------------------------|-----------------------------|
| $\delta\mathcal{L}^1$ (BH Theory) | -0.39 | -0.19 |
| $\delta\mathcal{L}^2$ (e^+ 94-97) | -0.46 | -0.66 |
| $\delta\mathcal{L}^3$ (e^- 98-99) | -0.69 | -1.20 |
| $\delta\mathcal{L}^4$ (e^+ 99-00) | -0.07 | -0.10 |
| $\delta\mathcal{L}^5$ (QEDC) | 0.81 | 1.70 |
| $\delta\mathcal{L}^6, \delta\mathcal{L}^7$ ($e^+ L + R$) | 0.84 | 0.80 |
| $\delta\mathcal{L}^8, \delta\mathcal{L}^9$ ($e^- L + R$) | 0.84 | 0.89 |

Precision medium Q^2
HERA-I data ~unshifted

New high Q^2 HERA-II
data shifted by ~1.7%
(less than 1 std.dev)

H1 Systematic Error Source Correlation



| Data set | $\delta\mathcal{L}$ | δE | $\delta\theta$ | δh | δN | δB | δV | δS | δpol |
|------------------------------|-----------------------|--|----------------|------------------|--------------|--------------|--------------|--------------|--------------------|
| e^+ Combined low Q^2 | $\delta\mathcal{L}^1$ | | | | | | | | |
| e^+ Combined low E_p | $\delta\mathcal{L}^1$ | | | | | | | | |
| e^+ NC 94-97 | $\delta\mathcal{L}^1$ | $\delta\mathcal{L}^2$ | δE^1 | $\delta\theta^1$ | δh^1 | δN^1 | δB^1 | — | — |
| e^+ CC 94-97 | $\delta\mathcal{L}^1$ | $\delta\mathcal{L}^2$ | — | — | δh^1 | δN^1 | δB^1 | δV^1 | — |
| e^- NC 98-99 | $\delta\mathcal{L}^1$ | $\delta\mathcal{L}^3$ | δE^1 | $\delta\theta^2$ | δh^1 | δN^1 | δB^1 | — | — |
| e^- NC 98-99 <i>high y</i> | $\delta\mathcal{L}^1$ | $\delta\mathcal{L}^3$ | δE^1 | $\delta\theta^2$ | δh^1 | δN^1 | — | — | δS^1 |
| e^- CC 98-99 | $\delta\mathcal{L}^1$ | $\delta\mathcal{L}^3$ | — | — | δh^1 | δN^1 | δB^1 | δV^2 | — |
| e^+ NC 99-00 | $\delta\mathcal{L}^1$ | $\delta\mathcal{L}^4$ | δE^1 | $\delta\theta^2$ | δh^1 | δN^1 | δB^1 | — | δS^1 |
| e^+ CC 99-00 | $\delta\mathcal{L}^1$ | $\delta\mathcal{L}^4$ | — | — | δh^1 | δN^1 | δB^1 | δV^2 | — |
| e^+ NC <i>high y</i> | $\delta\mathcal{L}^5$ | $\delta\mathcal{L}^6, \delta\mathcal{L}^7$ | δE^2 | $\delta\theta^3$ | δh^2 | δN^2 | — | — | δS^2 |
| e^- NC <i>high y</i> | $\delta\mathcal{L}^5$ | $\delta\mathcal{L}^8, \delta\mathcal{L}^9$ | δE^2 | $\delta\theta^3$ | δh^2 | δN^2 | — | — | δS^2 |
| e^+ NC <i>L</i> | $\delta\mathcal{L}^5$ | $\delta\mathcal{L}^6$ | δE^2 | $\delta\theta^3$ | δh^2 | δN^2 | δB^1 | — | δP^1 |
| e^+ CC <i>L</i> | $\delta\mathcal{L}^5$ | $\delta\mathcal{L}^6$ | — | — | δh^2 | δN^3 | δB^1 | δV^3 | δP^1 |
| e^+ NC <i>R</i> | $\delta\mathcal{L}^5$ | $\delta\mathcal{L}^7$ | δE^2 | $\delta\theta^3$ | δh^2 | δN^2 | δB^1 | — | δP^2 |
| e^+ CC <i>R</i> | $\delta\mathcal{L}^5$ | $\delta\mathcal{L}^7$ | — | — | δh^2 | δN^3 | δB^1 | δV^3 | δP^2 |
| e^- NC <i>L</i> | $\delta\mathcal{L}^5$ | $\delta\mathcal{L}^8$ | δE^2 | $\delta\theta^3$ | δh^2 | δN^2 | δB^1 | — | δP^3 |
| e^- CC <i>L</i> | $\delta\mathcal{L}^5$ | $\delta\mathcal{L}^8$ | — | — | δh^2 | δN^3 | δB^1 | δV^3 | δP^3 |
| e^- NC <i>R</i> | $\delta\mathcal{L}^5$ | $\delta\mathcal{L}^9$ | δE^2 | $\delta\theta^3$ | δh^2 | δN^2 | δB^1 | — | δP^4 |
| e^- CC <i>R</i> | $\delta\mathcal{L}^5$ | $\delta\mathcal{L}^9$ | — | — | δh^2 | δN^3 | δB^1 | δV^3 | δP^4 |

correlation of H1 systematic error sources

$\delta\mathcal{L}^1 \rightarrow 0.5\%$ BH theoretical error
HERA-I

$\delta\mathcal{L}^5 \rightarrow 2.3\%$ Compton lumi error
HERA-II

$\delta\mathcal{L}^{6-9} \rightarrow 1.5\%$ Compton unc. error
HERA-II

| Data Period | Global Normalisation | Per Period Normalisation | Total Normalisation |
|--------------------------|-------------------------|-----------------------------|------------------------|
| e^+ Combined low Q^2 | 0.993 | — | 0.993 |
| e^+ Combined low E_p | 0.993 | — | 0.993 |
| HERA I e^+ 94-97 | 0.993 | 0.999 | 0.992 |
| HERA I e^- 98-99 | 0.993 | 1.003 | 0.996 |
| HERA I e^+ 99-00 | 0.993 | 1.005 | 0.998 |
| HERA II e^+ L | 1.029 | 0.991 | 1.020 |
| HERA II e^+ R | 1.029 | 1.013 | 1.042 |
| HERA II e^- L | 1.029 | 1.010 | 1.039 |
| HERA II e^- R | 1.029 | 1.014 | 1.043 |

normalisations from H1PDF 2012

Low Q^2 data shifted by -0.7%
 HERA-I high Q^2 by -0.3%
 HERA-II high Q^2 by +2 to +4%

All shifts are <1.3 std.devs

HERAPDF1.0

Combine NC and CC HERA-I data from H1 & ZEUS
 Complete MSbar NLO fit
 NLO: standard parameterisation with 10 parameters
 $\alpha_s = 0.1176$ (fixed in fit)

HERAPDF1.5

Include additional NC and CC HERA-II data
 Complete MSbar NLO and NNLO fit
 NLO: standard parameterisation with 10 parameters
HERAPDF1.5f

NNLO: extended fit with 14 parameters

desy-09-158

H1-10-142 / ZEUS-prel-10-018

$$xf(x, Q_0^2) = A \cdot x^B \cdot (1-x)^C \cdot (1 + Dx + Ex^2)$$

| | | | | |
|------------|-------------------|----------------------------------|-------------------|--|
| xg | | xg | | $xg(x) = A_g x^{B_g} (1-x)^{C_g},$ |
| xu_v | | $xU = xu + xc$ | | $xu_v(x) = A_{u_v} x^{B_{u_v}} (1-x)^{C_{u_v}} (1 + E_{u_v} x^2),$ |
| xd_v | \longrightarrow | $xD = xd + xs$ | \longrightarrow | $xd_v(x) = A_{d_v} x^{B_{d_v}} (1-x)^{C_{d_v}},$ |
| $x\bar{U}$ | | $x\bar{U} = x\bar{u} + x\bar{c}$ | | $x\bar{U}(x) = A_{\bar{U}} x^{B_{\bar{U}}} (1-x)^{C_{\bar{U}}},$ |
| $x\bar{D}$ | | $x\bar{D} = x\bar{d} + x\bar{s}$ | | $x\bar{D}(x) = A_{\bar{D}} x^{B_{\bar{D}}} (1-x)^{C_{\bar{D}}}.$ |

$x\bar{s} = f_s x\bar{D}$ strange sea is a fixed fraction f_s of \bar{D} at Q_0^2

Apply momentum/counting sum rules:

$$\int_0^1 dx \cdot (xu_v + xd_v + x\bar{U} + x\bar{D} + xg) = 1$$

$$\int_0^1 dx \cdot u_v = 2 \quad \int_0^1 dx \cdot d_v = 1$$

Parameter constraints:

$$B_{uv} = B_{dv}$$

$$B_{Ubar} = B_{Dbar}$$

$$\text{sea} = 2 \times (\text{Ubar} + \text{Dbar})$$

$$\text{Ubar} = \text{Dbar at } x=0$$

$$Q_0^2 = 1.9 \text{ GeV}^2 \text{ (below } m_c)$$

$$Q^2 > 3.5 \text{ GeV}^2$$

$$2 \times 10^{-4} < x < 0.65$$

Fits performed using RT-VFNS

HERAPDF1.0 central values:

| | <i>A</i> | <i>B</i> | <i>C</i> | <i>E</i> |
|------------|----------|----------|----------|----------|
| xg | 6.8 | 0.22 | 9.0 | 9.7 |
| xu_v | 3.7 | 0.67 | 4.7 | |
| xd_v | 2.2 | 0.67 | 4.3 | |
| $x\bar{U}$ | 0.113 | -0.165 | 2.6 | |
| $x\bar{D}$ | 0.163 | -0.165 | 2.4 | |

$$\chi^2/\text{ndf} = 574/582$$

Experimental systematic sources of uncertainty allowed to float in fit
Include model assumptions into uncertainty:

f_s , m_c , m_b , Q_0^2 , Q_{min}^2

| Variation | Standard Value | Lower Limit | Upper Limit |
|---------------------------------|----------------|---------------------|----------------------|
| f_s | 0.31 | 0.23 | 0.38 |
| m_c [GeV] | 1.4 | 1.35 ^(a) | 1.65 |
| m_b [GeV] | 4.75 | 4.3 | 5.0 |
| Q_{min}^2 [GeV ²] | 3.5 | 2.5 | 5.0 |
| Q_0^2 [GeV ²] | 1.9 | 1.5 ^(b) | 2.5 ^(c,d) |

^(a) $Q_0^2 = 1.8$

^(c) $m_c = 1.6$

^(b) $f_s = 0.29$

^(d) $f_s = 0.34$

Excellent consistency of input data allow standard statistical error definition:

$$\Delta\chi^2 = 1$$

Exclusive jet data required for free α_s fit
See talk of Krzysztof Nowak

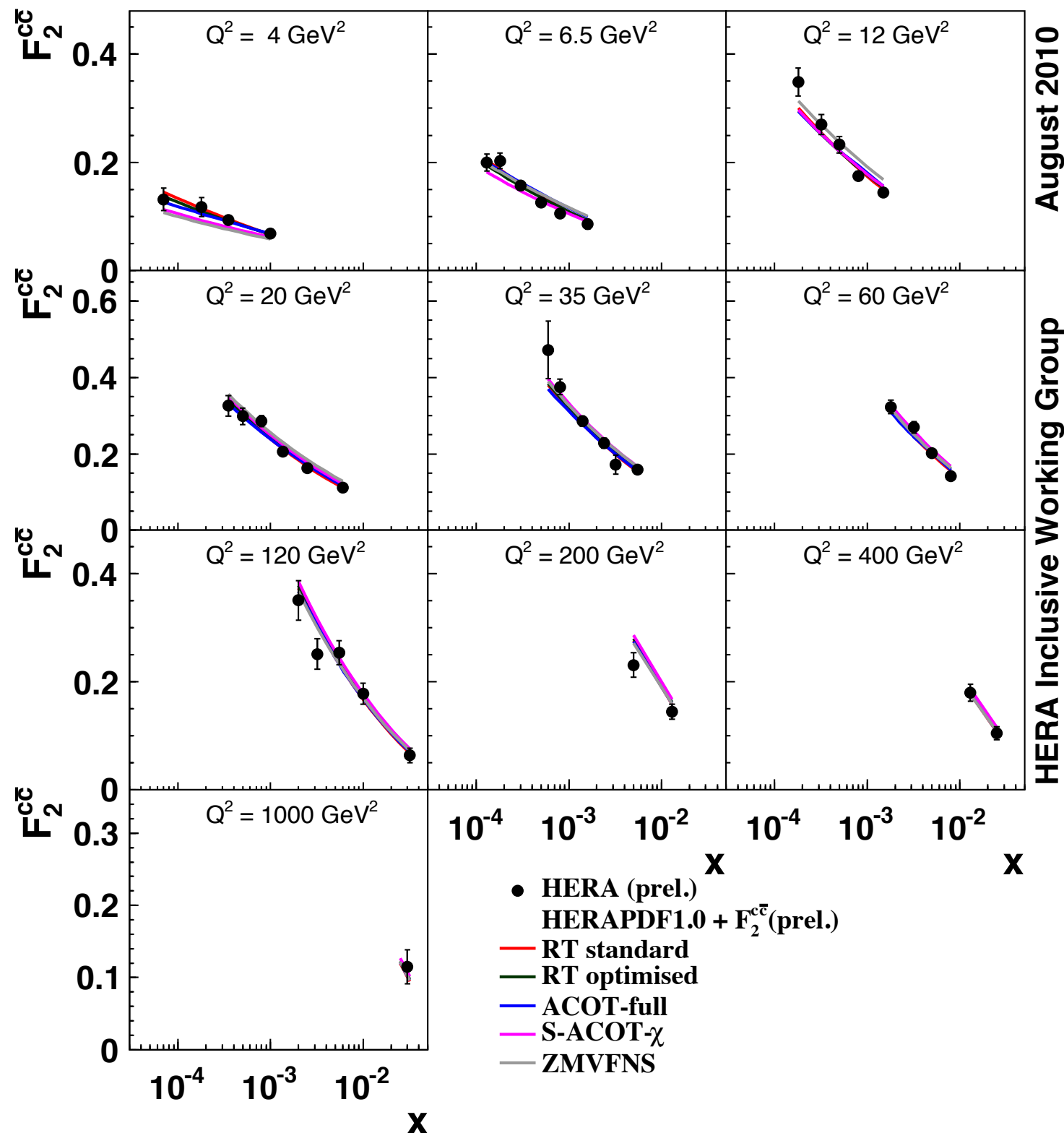
In 14 parameter fit:

release $B_{uv} = B_{dv}$ constraint

allow more flexible gluon

$$xg(x, Q_0^2) = A \cdot x^B \cdot (1-x)^C - A' \cdot x^{B'} \cdot (1-x)^{25}$$

allows for valence-like or negative gluon at Q_0^2



The inclusive charm content of proton can be measured in several methods:
 D^* decays , impact parameter significance...
 Combination yields $\sim 5\text{-}10\%$ precision

Data cover wide phase space region
 including charm threshold region

Theory predictions have small spread
 \Rightarrow use optimised m_c parameter

Spread of LHC Z/W production predictions is
 reduced $\sim 4.5\% \rightarrow \sim 0.7\%$
 when using optimal value of m_c